POLITECNICO DI TORINO
Repository ISTITUZIONALE

Guidelines and Recommendations on the Use of Higher OrderFinite Elements for Bending Analysis of Plates

Original
Guidelines and Recommendations on the Use of Higher OrderFinite Elements for Bending Analysis of Plates / Carrera, E., Miglioretti, F., Petrolo, M.. - In: INTERNATIONAL JOURNAL FOR COMPUTATIONAL METHODS IN ENGINEERING SCIENCE AND MECHANICS. - ISSN 1550-2287. - 12:(2011), pp. 303-324. [10.1080/15502287.2011.615792]

Availability:
This version is available at: 11583/2382508 since:

Publisher:
Taylor & Francis Group, LLC

Published
DOI:10.1080/15502287.2011.615792

Terms of use:

This article is made available under terms and conditions as specified in the corresponding bibliographic description in the repository

Publisher copyright
Taylor and Francis postprint/Author's Accepted Manuscript

This is an Accepted Manuscript of an article published by Taylor & Francis in INTERNATIONAL JOURNAL FOR COMPUTATIONAL METHODS IN ENGINEERING SCIENCE AND MECHANICS on 2011, available at http://wwww.tandfonline.com/10.1080/15502287.2011.615792

(Article begins on next page)

09 November 2026

Guidelines and Recommendations on the Use of Higher Order Finite Elements for Bending Analysis of Plates

E. Carrera,[1] F. Miglioretti,[1,2] and M. Petrolo[1]

[1]*Department of Aeronautic and Space Engineering, Politecnico di Torino, Torino, Italy*
[2]*Universite Paris Ouest Nanterre La Defense, Paris 10, France*

This paper compares and evaluates various plate finite elements to analyse the static response of thick and thin plates subjected to different loading and boundary conditions. Plate elements are based on different assumptions for the displacement distribution along the thickness direction. Classical (Kirchhoff and Reissner-Mindlin), refined (Reddy and Kant), and other higher-order displacement fields are implemented up to fourth-order expansion. The Unified Formulation UF by the first author is used to derive finite element matrices in terms of fundamental nuclei which consist of 3 × 3 arrays. The MITC4 shear-locking free type formulation is used for the FE approximation. Accuracy of a given plate element is established in terms of the error vs. thickness-to-length parameter. A significant number of finite elements for plates are implemented and compared using displacement and stress variables for various plate problems. Reduced models that are able to detect the 3D solution are built and a Best Plate Diagram (BPD) is introduced to give guidelines for the construction of plate theories based on a given accuracy and number of terms. It is concluded that the UF is a valuable tool to establish, for a given plate problem, the most accurate FE able to furnish results within a certain accuracy range. This allows us to obtain guidelines and recommendations in building refined elements in the bending analysis of plates for various geometries, loadings, and boundary conditions.

Keywords Finite element, Refined theories, Plate model, Unified formulation

1. INTRODUCTION

The development of plate models represents one of the most important issues of structural analysis. The use of two-dimensional models, such as plates and shells, is traditionally preferred to the more computationally expensive three-dimensional models. Best-known papers are those by Euler [1], Bernoulli [2], Cauchy [3], Poisson [4], Kirchhoff [5], Saint-Venant [6], Love [7], Reissner [8], Mindlin [9], and Vlasov [10]. The three-dimensional deformation state is usually simplified by means of "axiomatic" hypotheses based on conjecture: the cross-section remains plane, the section/thickness deformation can be discarded, shear strains are negligible, etc. . . . Excellent reviews, which give a complete overview of existing Layer-Wise and Equivalent Single Layer theories are those by Ambartsumian [11], Librescu and Reddy [12], Grigolyuk and Kolikov [13], Kapania and Raciti [14, 15], Kapania [16], Noor [17–19], Reddy and Robbins [20], Carrera [21, 22], Qatu [23, 24], and the books by Librescu [25], Reddy [26], and Qatu [27].

A different approach to build a structural model is based on the so-called "asymptotic" method where approximated theories are defined by employing asymptotic-type expansions of unknown variables over the section (beam case), or thickness (plate/shell geometries). Well-known papers on this topic are those by Cicala [28], Fettahlioglu and Steele [29], Berdischevsky [30, 31], Widera et al. [32, 33], and Spencer et al. [34], and the monograph by Cicala [35] and Goldenweizer [36].

The axiomatic and asymptotic techniques have important advantages and drawbacks. The former does not require complex mathematical tools but can lead to quite cumbersome models and the convergence of increasing order terms to the 3D solution cannot be guaranteed. The latter represents a systematic and powerful tool but, especially in the case of multilayered structures, requires the analysis of several parameters to build the model (e.g. the length-to-thickness, stacking sequences, orthotropic ratios). Moreover, the convergence to 3D solutions is guaranteed when one of these parameters vanishes with a consequent lack of information regarding the analysis of thick structures, for instance. This work consists of a companion paper by Carrera and Petrolo [37] where a so-called asymptotic/axiomatic approach has been recently proposed on the basis of closed-form solutions. Here it was shown how asymptotic-like results can

Federico Miglioretti acknowledges Alenia Aeronautica Torino for the financial support of the present research. Marco Petrolo is supported by the Regione Piemonte project MICROCOST.

Address correspondence to E. Carrera, Professor of Aerospace Structures and Aeroelasticity, Department of Aeronautic and Space Engineering, Politecnico di Torino, Corso Duca degli Abruzzi 24, 10129 Torino, Italy. E-mail: erasmo.carrera@polito.it

be obtained starting from a higher-order axiomatic-based model and considering a wide variety of parameters. The present paper extends the technique proposed to the finite element method in order to be able to deal with arbitrary geometries, boundary conditions, and loadings.

The advent of the computational mechanics and the finite element method has enabled a vast number of problems related to complicated geometries and boundary conditions to be solved. Various plate elements are present in open literature, and a brief overview of recent papers is herein conducted. Ganapathi et al. [38] developed a new eight-node C° membrane element based on the Reissner-Mindlin plate theory to analyze moderately thick laminates. Polit and Touratier [39] presented a C^1 six-node triangular finite element for geometrical linear and non-linear elastic multilayered composite plates that are able to model both thin and moderately thick plates without the classical pathologies of finite elements. Touratier and Faye [40] proposed elements for moderately thick plates and curved shells. Carrera and Demasi [41, 42] developed a plate element for the accurate description of stress and strain fields in multilayered thick plates subject to static loadings by exploiting two different variational statements: the principle of virtual displacement (PVD) and the Reissner mixed variational theorem (RMVT). The derivation of finite element matrices and numerical assessments were presented. Complete overviews on this topic can be found in the articles by Kant and Swaminathan [43] and Carrera [44].

This work is embedded in the framework of the Carrera Unified Formulation (CUF), which was introduced by the first author during the last decade and deals with refined beam, plate, and shell models. More details and assessments can be found in Carrera et al. [44–47]. CUF allows us to deal with any-order models by considering the order as an input of the analysis since the governing equations, in both strong and weak form, are given stemming from a few "fundamental nuclei" whose form does not depend on either the order of the introduced approximations or on the choices made for the base functions in the thickness direction (for plates/shells) or over the section (for beams). The FE plate formulation proposed is based on MITC4, see Carrera and Brischetto [48].

In this paper, CUF is exploited to implement refined models for isotropic plates and determine the role of each displacement variable in the solution. A term is considered ineffective, i.e. negligible, if its absence does not affect the accuracy of the solution with respect to a reference 3D solution. Reduced kinematic models, based on a set of retained displacement variables, are then obtained for each considered configuration. Moreover, a Best Plate Diagram (BPD) is proposed that gives guidelines to build plate theories with a given accuracy and a reduced number of displacement variables. The combined effect of loading and boundary conditions is evaluated. The paper has been organized as follows: a brief description of the adopted CUF formulation is given in Sections 2, 3, and 4; the method used to evaluate the effectiveness of various plate theories is introduced in Section 5; numerical results are provided in Section 6 and the main conclusions are outlined in Section 7.

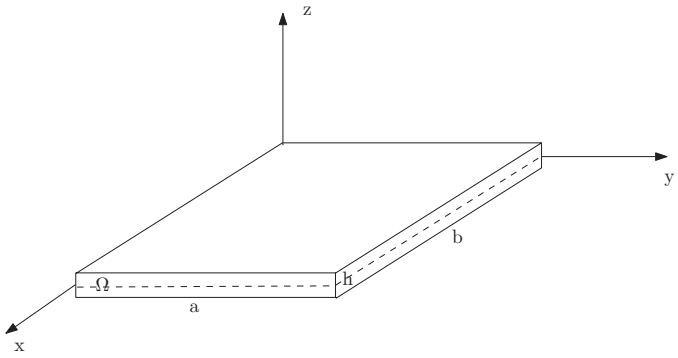

FIG. 1. Plate geometry.

2. PRELIMINARIES

The coordinate reference frame is shown in Fig. 1, x and y are the in-plane coordinates while z is the thickness. The displacement vector, $\mathbf{u}$, is:

$$\mathbf{u}(x, y, z) = \{ u_x \;\; u_y \;\; u_z \}^T, \tag{1}$$

the superscript "T" represents the transposition operator. Stress and strain components are grouped as follows:

$$\begin{aligned} \boldsymbol{\sigma}_p &= \{\sigma_{xx} \; \sigma_{yy} \; \sigma_{xy}\}^T \qquad \epsilon_p = \{\epsilon_{xx} \; \epsilon_{yy} \; \epsilon_{xy}\}^T \\ \boldsymbol{\sigma}_n &= \{\sigma_{xz} \; \sigma_{yz} \; \sigma_{zz}\}^T \qquad \epsilon_n = \{\epsilon_{xz} \; \epsilon_{yz} \; \epsilon_{zz}\}^T, \end{aligned} \tag{2}$$

where p indicates the in-plane components and n the out-of-plane components. Linear strain-displacement relations are used:

$$\begin{aligned} \epsilon_p &= \boldsymbol{D}_p \boldsymbol{u} \\ \epsilon_n &= \boldsymbol{D}_n \boldsymbol{u} = (\boldsymbol{D}_{n\Omega} + \boldsymbol{D}_{nz})\, \boldsymbol{u}, \end{aligned} \tag{3}$$

where:

$$\boldsymbol{D}_p = \begin{bmatrix} \dfrac{\partial}{\partial x} & 0 & 0 \\ 0 & \dfrac{\partial}{\partial y} & 0 \\ \dfrac{\partial}{\partial y} & \dfrac{\partial}{\partial x} & 0 \end{bmatrix} \quad \boldsymbol{D}_{n\Omega} = \begin{bmatrix} 0 & 0 & \dfrac{\partial}{\partial x} \\ 0 & 0 & \dfrac{\partial}{\partial y} \\ 0 & 0 & 0 \end{bmatrix}$$

$$\boldsymbol{D}_{nz} = \begin{bmatrix} \dfrac{\partial}{\partial z} & 0 & 0 \\ 0 & \dfrac{\partial}{\partial z} & 0 \\ 0 & 0 & \dfrac{\partial}{\partial z} \end{bmatrix}. \tag{4}$$

Hooke's law is used to compute stress components:

$$\boldsymbol{\sigma} = \boldsymbol{C}\boldsymbol{\epsilon}. \tag{5}$$

According to Eq. 2, the previous equation becomes:

$$\begin{aligned}\boldsymbol{\sigma}_p &= \boldsymbol{C}_{pp}\boldsymbol{\epsilon}_p + \boldsymbol{C}_{pn}\boldsymbol{\epsilon}_n \\ \sigma_n &= \boldsymbol{C}_{np}\boldsymbol{\epsilon}_p + \boldsymbol{C}_{nn}\boldsymbol{\epsilon}_n,\end{aligned} \tag{6}$$

where the material matrices are grouped as follows:

$$\boldsymbol{C}_{pp} = \begin{bmatrix} C_{11} & C_{12} & 0 \\ C_{21} & C_{22} & 0 \\ 0 & 0 & C_{66} \end{bmatrix} \quad \boldsymbol{C}_{nn} = \begin{bmatrix} C_{55} & 0 & 0 \\ 0 & C_{44} & 0 \\ 0 & 0 & C_{33} \end{bmatrix}$$

$$\boldsymbol{C}_{pn} = \boldsymbol{C}_{np}{}^T = \begin{bmatrix} 0 & 0 & C_{13} \\ 0 & 0 & C_{23} \\ 0 & 0 & 0 \end{bmatrix}. \tag{7}$$

The C_{ij} components are:

$$\begin{aligned}C_{11} &= C_{22} = C_{33} = \lambda + 2\mu \\ C_{12} &= C_{23} = C_{23} = \lambda \\ C_{44} &= C_{55} = C_{66} = \mu,\end{aligned} \tag{8}$$

where

$$\begin{aligned}\mu \equiv G &= \frac{E}{2(1+\nu)} \\ \lambda &= \frac{\nu E}{(1+\nu)(1-2\nu)}.\end{aligned} \tag{9}$$

Eq. 6 is used in the numerical analysis reported in this paper. Notice that the present plate formulation is not restricted to the isotropic case; it is also applicable to anisotropic laminates.

3. CARRERA UNIFIED FORMULATION

In the framework of the Carrera Unified Formulation, the displacement field along the thickness direction is expressed as an expansion of generic functions, F_τ:

$$\boldsymbol{u} = F_\tau \boldsymbol{u}_\tau \qquad \tau = 0, 1, \ldots, N, \tag{10}$$

where $\boldsymbol{u}_\tau$ is the displacement vector, F_τ are base functions of z, and N is the order of the expansion. Different base functions can be used; Taylor-like polynomials are used in this work:

$$F_\tau = z^\tau \qquad \tau = 0, 1, \ldots, N. \tag{11}$$

Any-order displacement fields can be adopted; a fourth-order model, for example, is defined by:

$$\begin{aligned}u_x &= u_{x0} + z u_{x1} + z^2 u_{x2} + z^3 u_{x3} + z^4 u_{x4} \\ u_y &= u_{y0} + z u_{y1} + z^2 u_{y2} + z^3 u_{y3} + z^4 u_{y4} \\ u_z &= u_{z0} + z u_{z1} + z^2 u_{z2} + z^3 u_{z3} + z^4 u_{z4}.\end{aligned} \tag{12}$$

Classical plate theories can be obtained from the linear expansion. The Reissner-Mindlin plate model approximation (see Reissner and Mindlin [8, 9]), also known as First Order Shear Deformation Theory, FSDT, in the case of laminates, requires two conditions: 1) First-order approximation kinematic fields; 2) the displacement component u_z has to be constant above the cross-section, i.e. $u_{z_1} = 0$. The resultant displacement model is:

$$\begin{aligned}u_x &= u_{x_0} + z\, u_{x_1} \\ u_y &= u_{y_0} + z\, u_{y_1} \\ u_z &= u_{z_0}.\end{aligned} \tag{13}$$

The Kirchhoff-type approximation (see [5]), also known as Classical Laminate Theory or CLT, can also be obtained using a penalty technique for the shear correction factor. First-order models require the use of reduced material stiffness coefficients to correct the thickness locking (see Carrera and Brischetto [49, 50]). Higher-order theories from open literature can also be obtained via CUF. Some of these models are considered in this paper for comparison purposes. They are obtained via CUF. According to Pandya (see [51]), the displacement components are given by:

$$\begin{aligned}u_x &= u_{x0} + z\, u_{x1} + z^2\, u_{x2} + z^3\, u_{x3} \\ u_y &= u_{y0} + z\, u_{y1} + z^2\, u_{y2} + z^3\, u_{y3} \\ u_z &= u_{z0}.\end{aligned} \tag{14}$$

Kant (see [52]) also expanded the displacement component $u_z(x, y, z)$ in Taylor's series of the thickness coordinate (hereinafter referred to as Kant-1):

$$\begin{aligned}u_x &= u_{x0} + z\, u_{x1} + z^2\, u_{x2} + z^3\, u_{x3} \\ u_y &= u_{y0} + z\, u_{y1} + z^2\, u_{y2} + z^3\, u_{y3} \\ u_z &= u_{z0} + z\, u_{z1} + z^2\, u_{z2} + z^3\, u_{z3}.\end{aligned} \tag{15}$$

Another Kant model (see [53]) is considered in this work (hereinafter referred to as Kant-2):

$$\begin{aligned}u_x &= z\, u_{x1} + z^3\, u_{x3} \\ u_y &= z\, u_{y1} + z^3\, u_{y3} \\ u_z &= u_{z0} + z^2\, u_{z2}.\end{aligned} \tag{16}$$

It is important to underline that CUF allows us to choose the higher-order terms to be included with no restrictions. For instance, one can consider a plate theory where incomplete fourth-order expansions are adopted:

$$\begin{aligned}u_x &= \quad + z\, u_{x1} + \quad + z^3\, u_{x3} + z^4\, u_{x4} \\ u_y &= \quad + z\, u_{y1} + z^2\, u_{y2} + \quad + z^4\, u_{y4} \\ u_z &= u_{z0} + z\, u_{z1} + z^2\, u_{z2} + \quad + z^4\, u_{z4}.\end{aligned} \tag{17}$$

4. FE GOVERNING EQUATIONS

The shape functions, N_i, and the nodal displacement vector, $\mathbf{q}_{\tau\mathbf{i}}$, are introduced to rewrite the displacement vector $\mathbf{u}_\tau$:

$$\mathbf{q}_{\tau\mathbf{i}} = \{q_{u_{x_{\tau i}}}\ q_{u_{y_{\tau i}}}\ q_{u_{z_{\tau i}}}\}^T \tag{18}$$

$$\mathbf{u} = N_i F_\tau \mathbf{q}_{\tau i}. \tag{19}$$

For the sake of brevity, the shape functions are not reported here. The four-node plate element with an assumed shear strain field concept of MITC4 type (see [54]) is adopted in this paper. The extension of the MITC4 element to the Unified Formulation has already been discussed in Carrera et al. [55].

Upon substitution of Eq. (19) in Eq. (3) it is possible to obtain:

$$\begin{aligned}\epsilon_p &= F_\tau \mathbf{D}_p(N_i\mathbf{I})\mathbf{q}_{\tau i}\\ \epsilon_n &= F_\tau \mathbf{D}_{n\Omega}(N_i\mathbf{I})\mathbf{q}_{\tau i} + F_{\tau,z}N_i\mathbf{q}_{\tau i},\end{aligned} \tag{20}$$

where $\boldsymbol{I}$ stands for the identity matrix. The stiffness matrix of the elements and the external loadings, which are consistent with the model, are obtained via the Principle of Virtual Displacements:

$$\delta L_{int} = \int_V \left(\delta\epsilon_p^T\sigma_p + \delta\epsilon_n^T\sigma_n\right) dV = \delta L_{ext}, \tag{21}$$

where L_{int} stands for the strain energy, and L_{ext} is the work of the external loadings. δ stands for the virtual variation. The virtual variation of the strain energy is rewritten using Eqs. (3), (6), and (19), so in a compact format it becomes:

$$\delta L_{int} = \delta\mathbf{q}_{\tau i}^T \mathbf{K}^{ij\tau s}\mathbf{q}_{sj}, \tag{22}$$

where $\mathbf{K}^{ij\tau s}$ is the stiffness matrix in the form of the fundamental nucleus. The following notation is introduced to indicate the line integrals along the thickness direction:

$$\begin{aligned}\left(\mathbf{Z}_{pp}^{\tau s}, \mathbf{Z}_{pn}^{\tau s}, \mathbf{Z}_{np}^{\tau s}, \mathbf{Z}_{nn}^{\tau s}\right) &= (\mathbf{C}_{pp}, \mathbf{C}_{pn}, \mathbf{C}_{np}, \mathbf{C}_{nn})E_{\tau s}\\ \left(\mathbf{Z}_{pn}^{\tau s_{,z}}, \mathbf{Z}_{nn}^{\tau s_{,z}}, \mathbf{Z}_{np}^{\tau_{,z} s}, \mathbf{Z}_{nn}^{\tau_{,z} s}, \mathbf{Z}_{nn}^{\tau_{,z} s_{,z}}\right) &= (\mathbf{C}_{pn}E_{\tau s_{,z}}, \mathbf{C}_{nn}E_{\tau s_{,z}}, \mathbf{C}_{np}E_{\tau_{,z} s},\\ &\qquad \mathbf{C}_{nn}E_{\tau_{,z} s}, \mathbf{C}_{nn}E_{\tau_{,z} s_{,z}})\\ (E_{\tau s}, E_{\tau s_{,z}}, E_{\tau_{,z} s}, E_{\tau_{,z} s_{,z}}) &= \int_A (F_\tau F_s, F_\tau F_{s_{,z}},\\ &\qquad F_{\tau_{,z}} F_s, F_{\tau_{,z}} F_{s_{,z}})dz.\end{aligned} \tag{23}$$

The compact expression of the stiffness matrix is then outlined:

$$\begin{aligned}\mathbf{K}^{\tau sij} = {} & \lhd \mathbf{D}_p^T(N_i\mathbf{I})\left[\mathbf{Z}_{pp}^{\tau s}\mathbf{D}_p(N_j\mathbf{I}) + \mathbf{Z}_{pn}^{\tau s}\mathbf{D}_{n\Omega}(N_j\mathbf{I}) + \mathbf{Z}_{pn}^{\tau s_{,z}}N_j\right]\\ & + \mathbf{D}_{n\Omega}^T(N_i\mathbf{I})[\mathbf{Z}_{np}^{\tau s}\mathbf{D}_p(N_j\mathbf{I}) + \mathbf{Z}_{nn}^{\tau s}\mathbf{D}_{n\Omega}(N_j\mathbf{I})\\ & + \mathbf{Z}_{nn}^{\tau s_{,z}}N_j] + N_i[\mathbf{Z}_{np}^{\tau_{,z} s}\mathbf{D}_p(N_j\mathbf{I}) + \mathbf{Z}_{nn}^{\tau_{,z} s}\mathbf{D}_{n\Omega}(N_j\mathbf{I})\\ & + \mathbf{Z}_{nn}^{\tau_{,z} s_{,z}}N_j] \rhd_\Omega .\end{aligned} \tag{24}$$

The symbols $\lhd \ldots \rhd_\Omega$ were introduced to denote integrals on Ω. The matrix $\mathbf{K}^{\tau sij}$ has 3×3 components and the 9 terms of $\mathbf{K}^{\tau sij}$ are:

$$\begin{aligned}K_{xx}^{\tau sij} &= Z_{pp11}^{\tau s} \lhd N_{i,x}N_{j,x} \rhd_\Omega + Z_{pp66}^{\tau s} \lhd N_{i,y}N_{j,y} \rhd_\Omega\\ &\quad + Z_{nn55}^{\tau_{,z} s_{,z}} \lhd N_iN_j \rhd_\Omega\\ K_{xy}^{\tau sij} &= Z_{pp12}^{\tau s} \lhd N_{i,x}N_{j,y} \rhd_\Omega + Z_{pp66}^{\tau s} \lhd N_{i,y}N_{j,x} \rhd_\Omega\\ K_{xz}^{\tau sij} &= Z_{pn13}^{\tau s_{,z}} \lhd N_{i,x}N_j \rhd_\Omega + Z_{nn55}^{\tau_{,z} s} \lhd N_iN_{j,x} \rhd_\Omega\\ K_{yx}^{\tau sij} &= Z_{pp12}^{\tau s} \lhd N_{i,y}N_{j,x} \rhd_\Omega + Z_{pp66}^{\tau s} \lhd N_{i,x}N_{j,y} \rhd_\Omega\\ K_{yy}^{\tau sij} &= Z_{pp22}^{\tau s} \lhd N_{i,y}N_{j,y} \rhd_\Omega + Z_{pp66}^{\tau s} \lhd N_{i,x}N_{j,x} \rhd_\Omega\\ &\quad + Z_{nn44}^{\tau_{,z} s_{,z}} \lhd N_iN_j \rhd_\Omega\\ K_{yz}^{\tau sij} &= Z_{pn23}^{\tau s_{,z}} \lhd N_{i,y}N_j \rhd_\Omega + Z_{nn44}^{\tau_{,z} s} \lhd N_iN_{j,y} \rhd_\Omega\\ K_{zx}^{\tau sij} &= Z_{nn55}^{\tau s_{,z}} \lhd N_{i,x}N_j \rhd_\Omega + Z_{np13}^{\tau_{,z} s} \lhd N_iN_{j,x} \rhd_\Omega\\ K_{zy}^{\tau sij} &= Z_{nn45}^{\tau s_{,z}} \lhd N_{i,x}N_j \rhd_\Omega + Z_{nn44}^{\tau s_{,z}} \lhd N_{i,y}N_j \rhd_\Omega\\ &\quad + Z_{np23}^{\tau_{,z} s} \lhd N_iN_{j,y} \rhd_\Omega\\ K_{zz}^{\tau sij} &= Z_{nn55}^{\tau s} \lhd N_{i,x}N_{j,x} \rhd_\Omega + Z_{nn44}^{\tau s} \lhd N_{i,y}N_{j,y} \rhd_\Omega\\ &\quad + Z_{nn33}^{\tau_{,z} s_{,z}} \lhd N_iN_j \rhd_\Omega .\end{aligned} \tag{25}$$

It should be noted that no assumptions on the approximation order were made. It is therefore possible to obtain refined plate models without changing the formal expression of the fundamental nucleus.

The loading vector, which is variationally consistent with the model, is derived in the case of a generic concentrate load $\boldsymbol{P}$:

$$\boldsymbol{P} = \{P_{u_x} \quad P_{u_y} \quad P_{u_z}\}. \tag{26}$$

Any other loading condition can be similarly treated as usual in FE applications. The virtual work due to $\boldsymbol{P}$ is:

$$\delta L_{ext} = \boldsymbol{P}\delta\boldsymbol{u}^T. \tag{27}$$

Substituting Eq. (19), the previous equation becomes:

$$\delta L_{ext} = F_\tau N_i \boldsymbol{P}\delta\boldsymbol{q}_{\tau i}^T. \tag{28}$$

This last equation permits the identification of the components of the nucleus which have to be loaded. In the case of a first-order expansion and $\boldsymbol{P}$ applied to a node and acting along the x direction, the virtual external work is:

$$\delta L_{ext} = P_{u_x}\delta u_{x1} + z_p P_{u_x}\delta u_{x2}, \tag{29}$$

where z_p is the thickness coordinate of the loading application point.

5. AN ASYMPTOTIC/AXIOMATIC APPROACH TO EVALUATE VARIOUS PLATE MODELS

Refined plate theories offer significant advantages in terms of accuracy of the solution and detection of non-classical effects. The drawback of these theories is that a higher computational cost has to be incurred because of the presence of a large number

TABLE 1
Locations of the displacement variables within the table layout

$N=0$	$N=1$	$N=2$	$N=3$	$N=4$
u_{x_0}	u_{x_1}	u_{x_2}	u_{x_3}	u_{x_4}
u_{y_0}	u_{y_1}	u_{y_2}	u_{y_3}	u_{y_4}
u_{z_0}	u_{z_1}	u_{z_2}	u_{z_3}	u_{z_4}

of displacement variables. The aim of this work is to better understand the influence of each term on the solution in order to evaluate which variables are effective and which are not. The effectiveness of each term is investigated as follows:

1. The problem data is fixed (i.e. geometry, boundary conditions, loadings, materials).
2. A set of output variables is chosen (e.g. maximum displacement, stress/displacement component at a given point).
3. A theory is fixed; that is, the terms that have to be considered in the expansion of u_x, u_y and u_z are established.
4. A reference solution is used to establish the accuracy (the $N=4$ case is assumed as the best-reference result).
5. CUF is used to generate the finite element solution for the theories considered.
6. The effectiveness of each term is numerically established by measuring the error produced with respect to the reference solution.
7. Any term that does not give any contribution to the computation of the mechanical response is not considered as effective in the plate model.
8. The most suitable plate model is then detected for a given structural layout; in other words, the plate model requiring the lowest number of terms to accomplish a give accuracy is built.

A graphic notation is introduced to make the representation of the obtained results more readable. Table 1 shows all the 15 terms of the expansion. The fourth-order model, $N=4$, is related to the following expression:

$$\begin{aligned} u_x &= u_{x0} + z u_{x1} + z^2 u_{x2} + z^3 u_{x3} + z^4 u_{x4} \\ u_y &= u_{y0} + z u_{y1} + z^2 u_{y2} + z^3 u_{y3} + z^4 u_{y4} \\ u_z &= u_{z0} + z u_{z1} + z^2 u_{z2} + z^3 u_{z3} + z^4 u_{z4}. \end{aligned} \tag{30}$$

The first three terms are constant (the first column), the second three terms are linear (the second column), the third three terms are quadratic (the third column), the fourth three terms are cubic

TABLE 2
Symbolic representation of the kinematic model with u_{y_2} deactivated

●	●	●	●	●
●	●	○	●	●
●	●	●	●	●

TABLE 3
Symbolic representation of the Kant [52] kinematic model

●	●	●	●	○
●	●	●	●	○
●	●	●	●	○

(the fourth column) and the last three terms are fourth-order displacement variables (the fifth column). The total number of expansion terms is 15. A set of symbols is used to denote the active and inactive terms. Each adopted symbol is related to a given structural case. The black color indicates that the term is active; that is, the displacement variable is exploited to compute the results while the white color indicates that the term is inactive; that is, the displacement variable is removed from the displacement model. Table 2 shows the case where the parabolic term of the in-plane displacement of the expansion in the y-direction is discarded. The explicit displacement model related to Table 2 is:

$$\begin{aligned} u_x &= u_{x0} + z u_{x1} + z^2 u_{x2} + z^3 u_{x3} + z^4 u_{x4} \\ u_y &= u_{y0} + z u_{y1} + \quad + z^3 u_{y3} + z^4 u_{y4} \\ u_z &= u_{z0} + z u_{z1} + z^2 u_{z2} + z^3 u_{z3} + z^4 u_{z4}. \end{aligned} \tag{31}$$

As a further example, Table 3 reports the schematic representation of the Kant-1 (15) plate model. The elimination of a term, as well as the evaluation of its effectiveness in the analysis, can be obtained either by rearranging the rows and columns of the stiffness matrix or by exploiting a penalty technique. The accuracy of a reduced model is evaluated by computing δ_u and δ_σ. These quantities are defined according to the following formulas:

$$\begin{aligned} \delta_{u_z} &= \frac{u_z}{u_{z_{ref}}} \times 100\% \\ \delta_{\sigma_{zz}} &= \frac{\sigma_{zz}}{\sigma_{zz_{ref}}} \times 100\%, \end{aligned} \tag{32}$$

where $u_{z_{ref}}$ and $\sigma_{zz_{ref}}$ denote the transversal displacement and stress values, which are taken as references. A displacement

TABLE 4
Symbols that indicate the status of a displacement variable for different boundary conditions: clamped, 'c', simply-supported, "s", free, "f"

Active term	Inactive term	
▲	△	$ssss$
■	□	$cfcf$
▼	▽	$cccc$
♦	◊	$scsc$

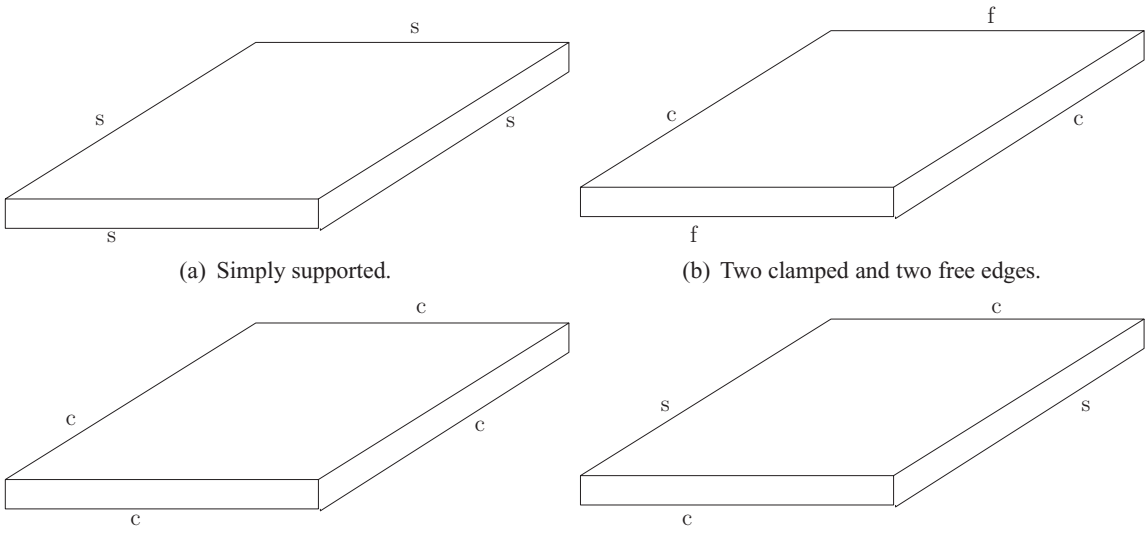

(a) Simply supported.

(b) Two clamped and two free edges.

(c) Four clamped edges.

(d) Two simply supported and two clamped edges.

FIG. 2. Adopted boundary conditions.

variable of the expansion is considered to be non-effective with respect to a specific output component when, if neglected (removed from the formulation), it does not introduce any changes in the results according to a fixed accuracy ($\delta \geq 99.95\%$). This value was chosen as it was observed that, if the reduced model that does not include the terms causing a loss in accuracy lower than 0.05% is considered, the loss in accuracy of the reduced model will be lower than 0.05% . A companion parameter that will be used is related to the error calculated. If u_z is considered, the error will be defined as:

$$error = \left\| \frac{u_z - u_{z_{ref}}}{u_{z_{ref}}} \right\| \times 100\%. \tag{33}$$

The approach described allows us to build plate models that are equivalent to a full higher-order model ($N = 4$ in this paper) having a lower number of displacement variables. A further analysis is then conducted on the reduced models by decreasing the fixed accuracy. This allows us to build a so-called Best Plate Diagram consisting of a "number of term vs. error," curve which can be useful to determine the effectiveness of a given theory in terms of accuracy and computational cost.

The asymptotic/axiomatic approach is herein applied by making different parameters vary. The influence of the following plate characteristics in determining a plate model is evaluated:

1. Boundary conditions.
2. Loadings.
3. The length-to-thickness ratio (a/h).

6. RESULTS AND DISCUSSION

An isotropic plate is considered. The Young modulus, E, is equal to 73 [GPa] and the Poisson ratio, ν, is equal to 0.34. The geometry of the plate is shown in Fig. 1, where a is 0.1 [m], and b is equal to a. u_z, σ_{xx}, σ_{yy}, and σ_{zz} are computed at [$a/2$, $b/2$, 0], while σ_{xz} is computed at [0, $b/2$, $h/2$] and σ_{yz} is computed at [$a/2$, 0, $h/2$]. Stresses are computed through Hooke's laws. Four-node plate elements have been used, and a uniform mesh of 15×15 elements has been adopted after a convergence study.

TABLE 5

Comparison of the the 3D model and the fourth-order FEM model solutions in the case of simply supported plate with a distributed load: $\bar{u}_z = u_z \frac{100 E_T h^3}{p_z a^4}$, $\bar{\sigma}_{xx} = \frac{\sigma_{xx}}{\bar{p}_z(a/h)}$, $\bar{\sigma}_{xz} = \frac{\sigma_{xz}}{\bar{p}_z(a/h)^2}$, $\bar{\sigma}_{zz} = \frac{\sigma_{zz}}{\bar{p}_z(a/h)}$

	$\bar{u}_{z_{N=4FEM}}$	$\bar{u}_{z_{3D}}$	$\bar{\sigma}_{xx_{N=4FEM}}$	$\bar{\sigma}_{xx_{3D}}$	$\bar{\sigma}_{xz_{N=4FEM}}$	$\bar{\sigma}_{xz_{3D}}$	$\bar{\sigma}_{zz_{N=4FEM}}$	$\bar{\sigma}_{zz_{3D}}$
$a/h = 100$	2.7134	2.7248	0.2040	0.2037	0.2390	0.2387	0.0866	0.0100
$a/h = 10$	2.8255	2.8345	0.2070	0.2068	0.2386	0.2383	0.1041	0.1000
$a/h = 5$	3.1978	3.2056	0.2172	0.2168	0.2378	0.2371	0.2024	0.2002
$a/h = 2$	7.3840	7.3826	0.3171	0.3145	0.2308	0.2277	0.5099	0.5000

TABLE 6

Influence of each displacement variable of a fourth-order model on the solution, simply supported plate with a distributed load, $a/h = 10$

	δ_{u_z} [%]	$\delta_{\sigma_{xx}}$ [%]	$\delta_{\sigma_{xz}}$ [%]	$\delta_{\sigma_{zz}}$ [%]
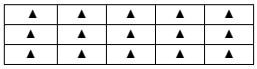	100.0	100.0	100.0	100.0
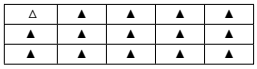	100.0	100.5	100.0	100.1
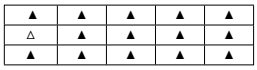	100.0	99.9	100.0	100.1
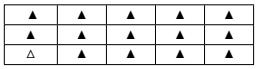	0.13	1.18	1.27	75.59
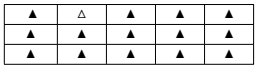	19.5	14.7	269.3	93.9
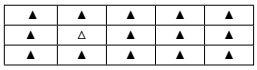	19.5	18.8	16.11	93.90
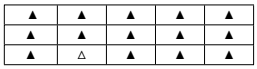	100.0	101.4	100.0	136.3
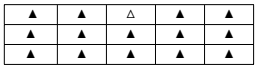	100.0	100.0	100.0	100.1
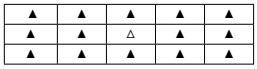	100.0	100.0	100.0	100.1
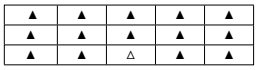	95.4	76.6	101.6	−598.1
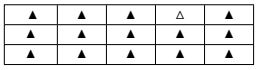	99.7	99.7	72.2	100.0
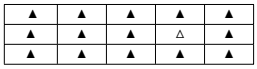	99.7	99.7	99.9	100.0
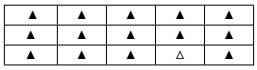	100.0	100.0	100.0	100.5
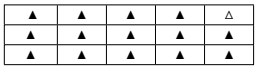	100.0	100.0	100.0	100.0

(Continued on next page)

TABLE 6
Influence of each displacement variable of a fourth-order model on the solution, simply supported plate with a distributed load, $a/h = 10$ *(Continued)*

	δ_{u_z} [%]	$\delta_{\sigma_{xx}}$ [%]	$\delta_{\sigma_{xz}}$ [%]	$\delta_{\sigma_{zz}}$ [%]
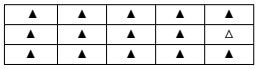	100.0	100.0	100.0	100.0
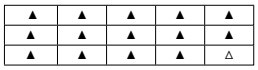	100.0	100.7	100.0	125.7

6.1. Boundary Condition Effects

The investigation of the role of each displacement variable under different boundary conditions is conducted as a first assessment. Four different boundary condition sets are considered:

1. *ssss*, four simply-supported edges;
2. *cf cf*, two clamped and two free edges;
3. *cccc*, four clamped edges;
4. *sc sc*, two simply-supported and two clamped edges.

TABLE 7
Comparison of the sets of effective terms for a plate with a distributed load with different boundary conditions, $a/h = 10$

	ssss	*cf cf*	*cccc*	*scsc*
u_z	$M_e = 6$ 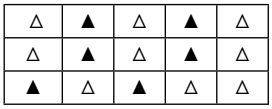	$M_e = 7$ 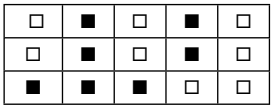	$M_e = 7$ 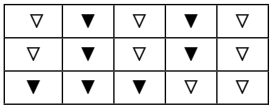	$M_e = 7$ 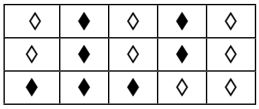
σ_{xx}	$M_e = 10$ 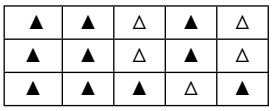	$M_e = 10$ 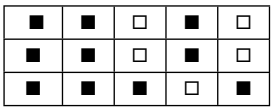	$M_e = 10$ 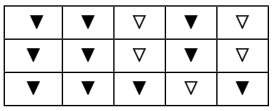	$M_e = 9$ 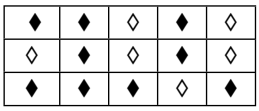
σ_{yy}	$M_e = 10$ 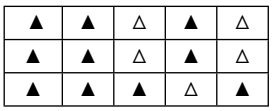	$M_e = 10$ 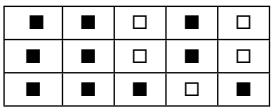	$M_e = 10$ 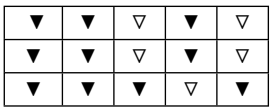	$M_e = 10$ 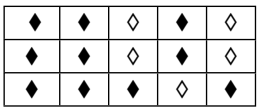
σ_{xz}	$M_e = 6$ 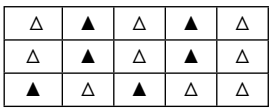	$M_e = 6$ 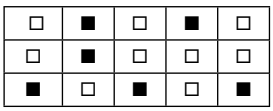	$M_e = 7$ 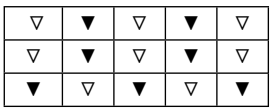	$M_e = 6$ 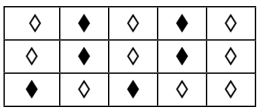
σ_{yz}	$M_e = 6$ 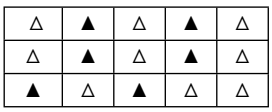	$M_e = 7$ 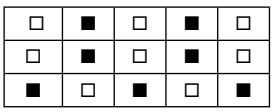	$M_e = 7$ 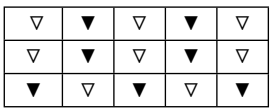	$M_e = 6$ 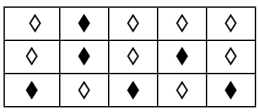
σ_{zz}	$M_e = 11$ 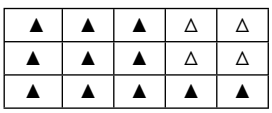	$M_e = 12$ 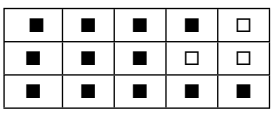	$M_e = 13$ 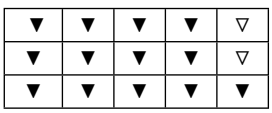	$M_e = 12$ 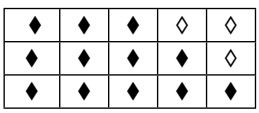
COMBINED	$M_e = 13$ 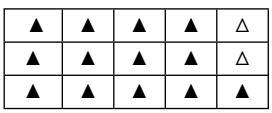	$M_e = 13$ 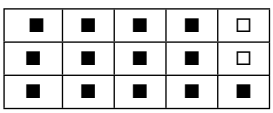	$M_e = 13$ 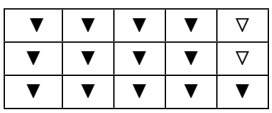	$M_e = 13$ 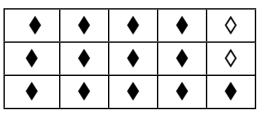

TABLE 8
Accuracy of different models for a plate with a distributed load, $a/h = 10$

	δ_{u_z} [%]	$\delta_{\sigma_{xx}}$ [%]	$\delta_{\sigma_{yy}}$ [%]	$\delta_{\sigma_{xz}}$ [%]	$\delta_{\sigma_{yz}}$ [%]	$\delta_{\sigma_{zz}}$ [%]
ssss						
▲ ▲ ▲ ▲ △ ▲ ▲ ▲ ▲ △ ▲ ▲ ▲ ▲ ▲	100.0	100.0	100.0	100.0	100.0	100.0
CPT	96.1	98.4	98.4	66.8	66.8	1974.2
FSDT	100.9	98.4	98.4	66.8	66.8	1974.2
Kant-2	99.9	100.2	100.2	100.0	100.0	79.4
cfcf						
■ ■ ■ ■ □ ■ ■ ■ ■ □ ■ ■ ■ ■ ■	100.0	100.0	100.0	100.0	100.0	100.0
CPT	91.2	98.3	94.9	239.5	−67.86	1171.3
FSDT	103.1	98.7	97.2	83.2	65.4	1183.7
Kant-2	99.9	100.0	101.0	98.8	99.7	80.4
scsc						
▼ ▼ ▼ ▼ ▽ ▼ ▼ ▼ ▼ ▽ ▼ ▼ ▼ ▼ ▼	100.0	100.0	100.0	100.0	100.0	100.0
CPT	88.4	96.2	96.2	87.5	87.5	1074.0
FSDT	102.8	97.1	97.1	81.4	81.4	1084.8
Kant-2	99.8	99.9	99.9	98.9	98.9	80.0
scsc						
♦ ♦ ♦ ♦ ◊ ♦ ♦ ♦ ♦ ◊ ♦ ♦ ♦ ♦ ♦	100.0	100.0	100.0	100.0	100.0	100.0
CPT	90.2	94.6	97.7	66.1	84.7	1281.1
FSDT	102.4	98.3	97.9	67.3	81.8	1304.3
Kant-2	99.8	100.6	100.0	100.0	98.9	79.8

Fig. 2 shows each set and Table 4 presents the relative symbolic representation, which is exploited to report the results in a compact manner. A bi-sinusoidal transverse distributed load is applied at the top surface. Its expression is:

$$P_z = p_z sin\left(\frac{mx}{a}\right) cos\left(\frac{ny}{b}\right), \tag{34}$$

where p_z is the amplitude and is equal to 1 [kPa]; m and n are the wave numbers in the two in-plane plate directions, both of them are equal to 1. A 3D solution is used to identify which order of the expansion has to be used to obtain 3D-like results; that is, which higher-order plate model is needed to detect a 3D exact solution. Table 5 shows the comparison of the 3D solution and the fourth-order FEM one. The fourth-order model solution, $N = 4$, offers an excellent match with the exact solution for

TABLE 9
Sets of effective terms for all the considered boundary conditions

▲■▼♦	▲■▼♦	▲■▼♦	▲■▼♦	△ □▽◊
▲■▼♦	▲■▼♦	▲■▼♦	▲■▼♦	△ □▽◊
▲■▼♦	▲■▼♦	▲■▼♦	▲■▼♦	▲■▼♦

TABLE 10
Symbols that indicate the status of a displacement variable for different loading conditions

Active term	Inactive term	
▲	△	*Distributed Load* 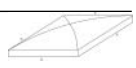
■	□	*Point Load* 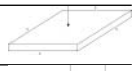
▼	▽	*Four Point Loads* 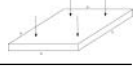

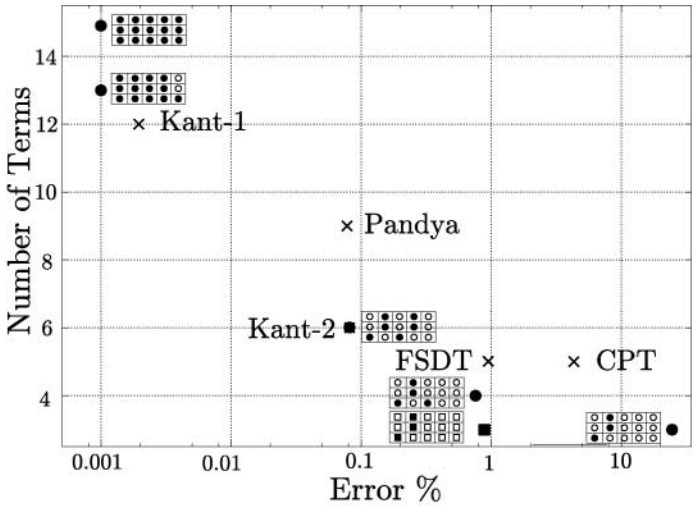

(a) Simply supported plate. Output u_z.

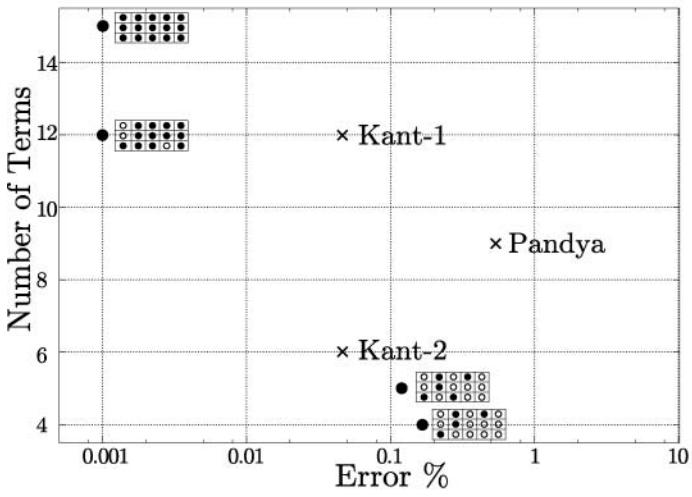

(b) Simply supported plate. Output σ_{xz}.

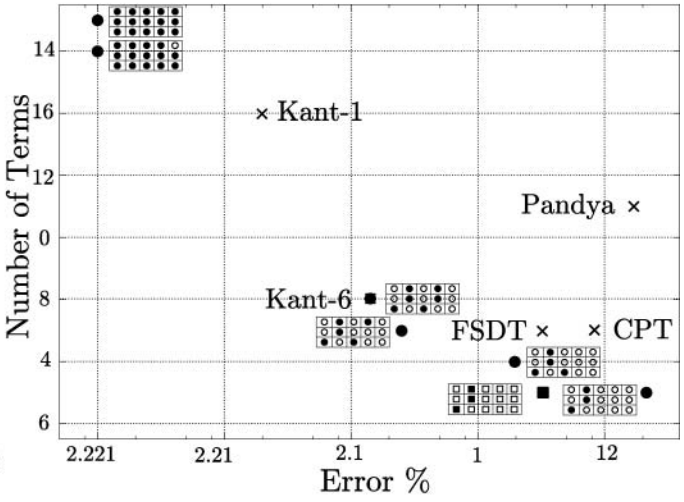

(c) Two clamped e two free edges plate. Output u_z.

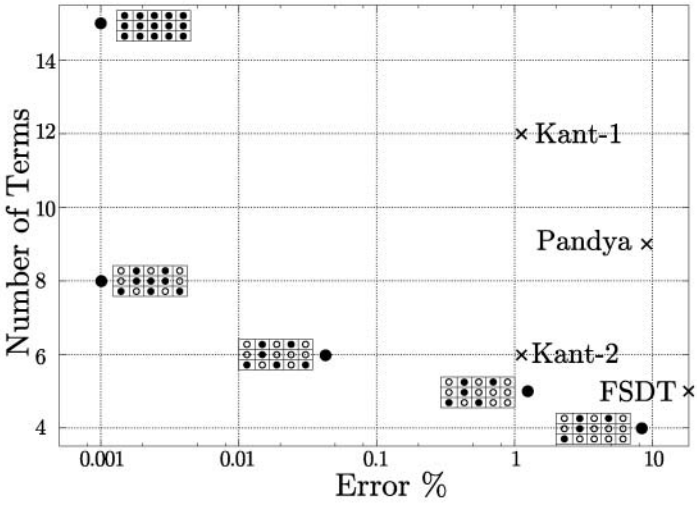

(d) Two clamped e two free edges plate. Output σ_{xz}.

FIG. 3. Number of terms vs. error for different output variables by various models for a simply supported plate and two edges free and two edges clamped plate with a distributed load, $a/h = 10$. ■ model with the thickness locking corrected.

TABLE 11

Fourth-order FEM model solutions in the case of simply supported plate subject to point loading conditions, $a/h = 10$

	$u_{z_{N=4}}$ [m]	$\sigma_{xx_{N=4}}$ [Pa]	$\sigma_{yz_{N=4}}$ [Pa]	$\sigma_{zz_{N=4}}$ [Pa]
Point Load	1.7662×10^{-7}	1.9336×10^{5}	7.0444×10^{3}	3.1373×10^{4}
Four Point Loads	1.7662×10^{-7}	1.9336×10^{5}	6.2392×10^{3}	3.1373×10^{4}

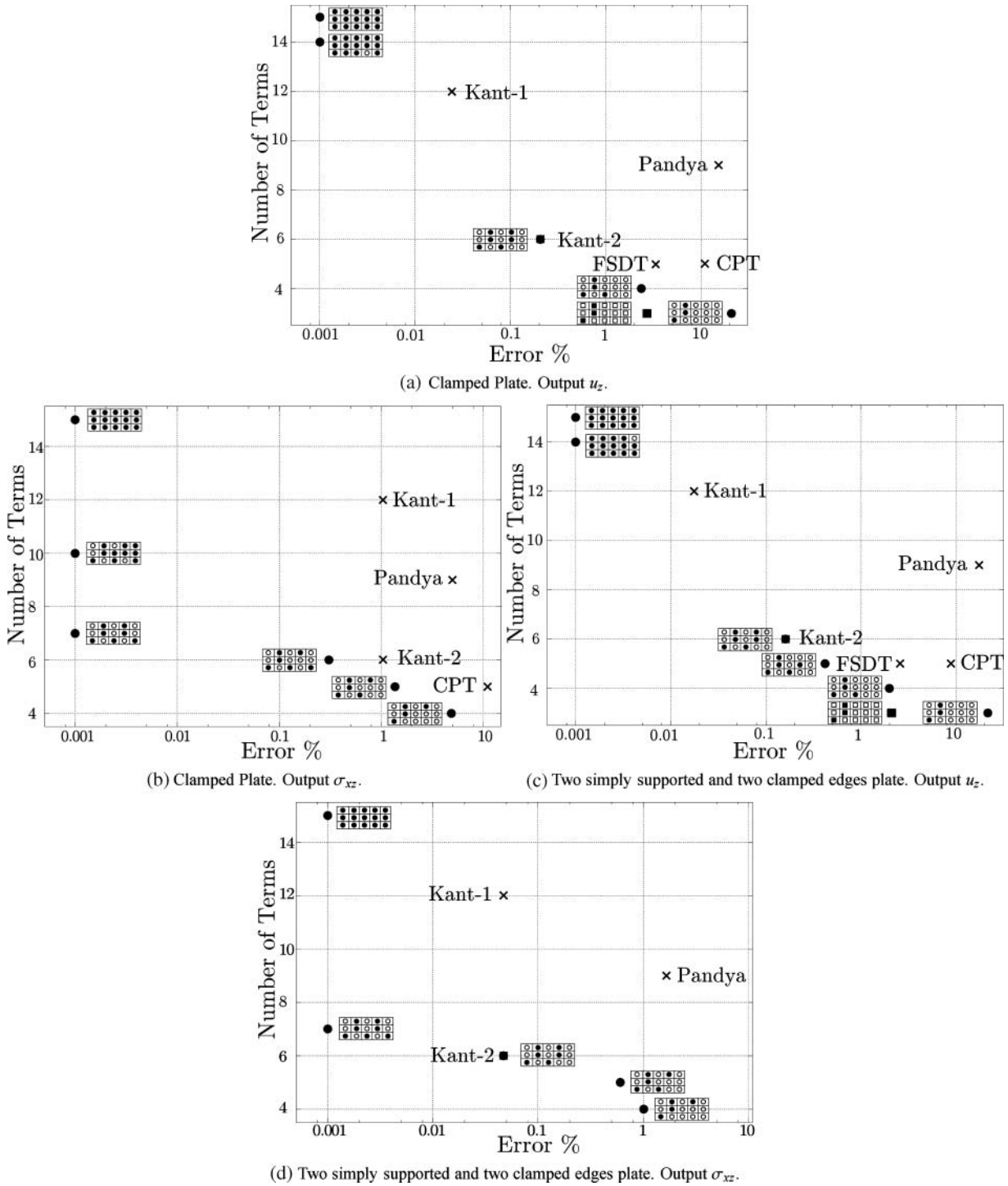

(a) Clamped Plate. Output u_z.

(b) Clamped Plate. Output σ_{xz}.

(c) Two simply supported and two clamped edges plate. Output u_z.

(d) Two simply supported and two clamped edges plate. Output σ_{xz}.

FIG. 4. Number of terms vs. error for different output variables by various models for a clamped plate and two simply-supported edges and two clamped edges plate with a distributed load, $a/h = 10$. ■ model with the thickness locking corrected.

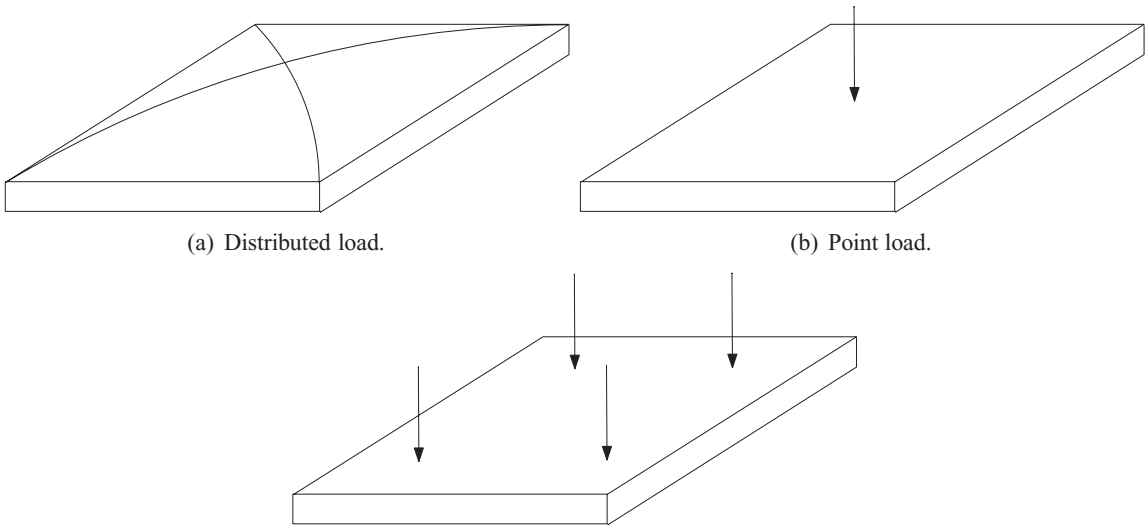

(a) Distributed load.

(b) Point load.

(c) Point loads.

FIG. 5. Adopted loading conditions.

about all the length-to-thickness ratios and considered outputs, therefore it has been chosen as the reference for the following analyses. The effectiveness of each term is investigated for each set of boundary conditions. Table 6 shows the analysis of a moderately thick simply-supported plate. The first column shows the plate models considered. The remaining columns report model accuracies in determining a given output variable compared to a full fourth-order model. Table 7 has been obtained by exploiting Table 6: the sets of displacement variables which are needed to exactly detect various output variables are given. Each row refers to an output variable. Each column considers a different set of boundary conditions. M_e indicates the number of terms (i.e. the computational cost) of the models that are equivalent to the fourth-order one. The last row shows the expansion terms needed to detect all the considered outputs. The latter combined models are used to build Table 8, which shows a comparison with the accuracies given by CPT, FSDT, and Kant-2 plate models. Table 9 summarizes the combined displacement fields that are needed to detect the exact solution for all the considered boundary conditions. The results that have been shown so far give us the reduced plate models, which detect a 3D-like solution. Starting from these reduced models, it is possible to determine further theories that provide solutions with a certain degree of error compared to the full fourth-order one. Fig. 3 and Fig. 4, show the number of terms needed to detect an output variable with a given error. The corresponding plate models are also indicated. For the linear models, the results are reported with and without the correction of the thickness locking. Models from the open literature have also been included. The accepted error range varies from 0% to 10%. The analyses undertaken suggest what follows:

1. The reduced plate models, which are equivalent to a fourth-order theory, vary significantly if different output variables are considered.
2. The influence of boundary conditions is not high.
3. Classical models are inadequate to deal with shear stresses.
4. A significant computational cost reduction is obtained only if a limited number of output variables has to be detected.
5. The number of terms vs. error diagram shows that all the theories derived from the present approach are able to satisfy a given error requirement with a lower computational cost than the open literature models considered. This shows the strength of the present technique for detecting the possible best theories for a given structural problem.

6.2. Loading Effects

The effect of the loading conditions is herein investigated. A simply supported plate is considered. Three different loading conditions are taken into account:

1. A bi-sinusoidal distributed load (Fig. 5 (a));
2. A point load (Fig. 5 (b));
3. Four point loads (Fig. 5 (c)).

The point load, which is applied at the top surface of the plate, has an intensity of 10 N while the four point loads have an intensity of 2.5 N each. Table 10 reports the symbolic representation of each loading set. Table 11 shows the fourth-order FEM solution for the point load condition. Table 5 values are used for

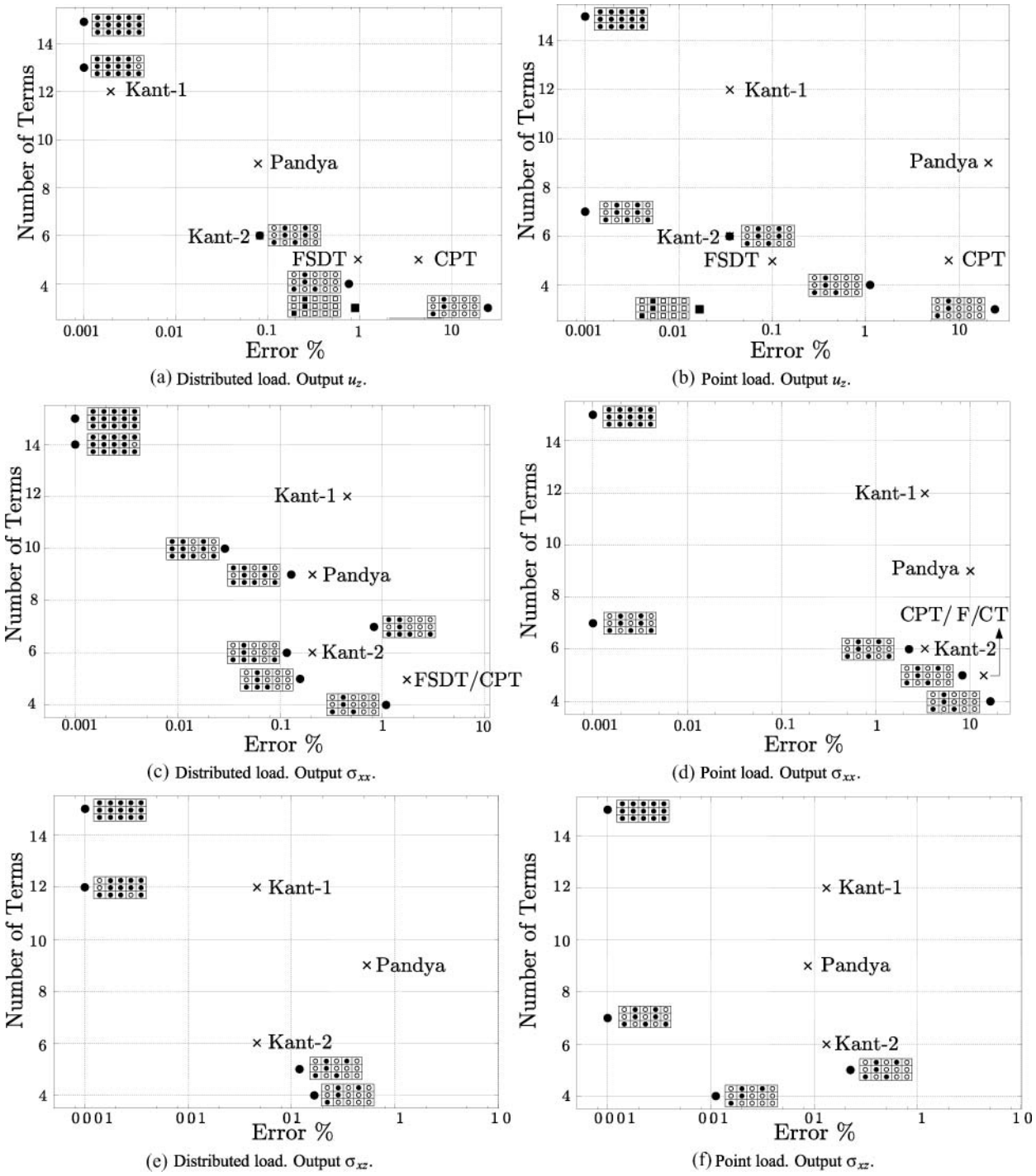

FIG. 6. Number of terms vs. error for different output variables and loading conditions by various models for a simply-supported plate, $a/h = 10$. ■ model with the thickness locking corrected.

the distributed loading case. The sets of displacement variables, which are needed to detect various outputs precisely, are given in Table 12. Each row refers to a different output variable. Each column considers a different loading condition. M_e indicates the number of terms of the models that are equivalent to the fourth-order one. The last row shows the plate models that are needed to detect all the considered outputs precisely. The latter combined models are used to build Table 13, which shows a comparison of the accuracies given by CPT, FSDT, and Kant-2 plate models. Table 14 summarizes the combined displacement fields, able to detect the exact solution for all the considered loading conditions. Fig. 6 shows the number of terms needed

TABLE 12
Comparison of the sets of effective terms for a simply supported plate subject to different loading conditions

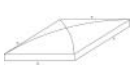
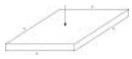
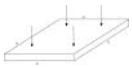

	$M_e = 6$	$M_e = 6$	$M_e = 6$
u_z	△ ▲ △ ▲ △ △ ▲ △ ▲ △ ▲ △ ▲ △ △	□ ■ □ ■ □ □ ■ □ ■ □ ■ □ ■ □ □	▽ ▼ ▽ ▼ ▽ ▽ ▼ ▽ ▼ ▽ ▼ ▽ ▼ ▽ ▽
	$M_e = 10$	$M_e = 7$	$M_e = 7$
σ_{xx}	▲ ▲ △ ▲ △ ▲ ▲ △ ▲ △ ▲ ▲ ▲ △ ▲	□ ■ □ ■ □ □ ■ □ ■ □ ■ □ ■ □ ■	▽ ▼ ▽ ▼ ▽ ▽ ▼ ▽ ▼ ▽ ▼ ▽ ▼ ▽ ▼
	$M_e = 10$	$M_e = 7$	$M_e = 7$
σ_{yy}	▲ ▲ △ ▲ △ ▲ ▲ △ ▲ △ ▲ ▲ ▲ △ ▲	□ ■ □ ■ □ □ ■ □ ■ □ ■ □ ■ □ ■	▽ ▼ ▽ ▼ ▽ ▽ ▼ ▽ ▼ ▽ ▼ ▽ ▼ ▽ ▼
	$M_e = 6$	$M_e = 7$	$M_e = 7$
σ_{xz}	△ ▲ △ ▲ △ △ ▲ △ ▲ △ ▲ △ ▲ △ △	□ ■ □ ■ □ □ ■ □ ■ □ ■ □ ■ □ ■	▽ ▼ ▽ ▼ ▽ ▽ ▼ ▽ ▼ ▽ ▼ ▽ ▼ ▽ ▼
	$M_e = 6$	$M_e = 7$	$M_e = 7$
σ_{yz}	△ ▲ △ ▲ △ △ ▲ △ ▲ △ ▲ △ ▲ △ △	□ ■ □ ■ □ □ ■ □ ■ □ ■ □ ■ □ ■	▽ ▼ ▽ ▼ ▽ ▽ ▼ ▽ ▼ ▽ ▼ ▽ ▼ ▽ ▼
	$M_e = 11$	$M_e = 7$	$M_e = 7$
σ_{zz}	▲ ▲ ▲ △ △ ▲ ▲ ▲ △ △ ▲ ▲ ▲ ▲ ▲	□ ■ □ ■ □ □ ■ □ ■ □ ■ □ ■ □ ■	▽ ▼ ▽ ▼ ▽ ▽ ▼ ▽ ▼ ▽ ▼ ▽ ▼ ▽ ▼
	$M_e = 13$	$M_e = 7$	$M_e = 7$
COMBINED	▲ ▲ ▲ ▲ △ ▲ ▲ ▲ ▲ △ ▲ ▲ ▲ ▲ ▲	□ ■ □ ■ □ □ ■ □ ■ □ ■ □ ■ □ ■	▽ ▼ ▽ ▼ ▽ ▽ ▼ ▽ ▼ ▽ ▼ ▽ ▼ ▽ ▼

to compute an output variable with a given error. The corresponding plate models are also indicated together with models retrieved from open literature. For the linear models, the results are reported with and without the thickness locking correction. The accepted error range varies from 0% to 10%. No differences between the one point load case and the four point load one have been observed; therefore the graphs related to the four point load are not reported. The following remarks arise from the analyses carried out:

1. The sets of effective displacement variables vary if distributed or concentrated loads are considered, whereas there are no differences if one or multiple point loads are used.
2. The effect of the considered output variable is significant in the case of distributed load, it is almost negligible if point loads are considered.
3. The validity of the number of terms vs. error diagram for providing guidelines for the construction of plate theories accomplishing a given accuracy is confirmed. As the error is fixed, the theories derived generally lie beneath classical and other refined models; that is, the proposed models are able to fulfill a certain accuracy demand with a lower computational cost.

TABLE 13
Accuracy of different plate models for a simply supported plate subject to various loading conditions, $a/h = 10$

	δ_{u_z} [%]	$\delta_{\sigma_{xx}}$ [%]	$\delta_{\sigma_{yy}}$ [%]	$\delta_{\sigma_{xz}}$ [%]	$\delta_{\sigma_{xz}}$ [%]	$\delta_{\sigma_{zz}}$ [%]
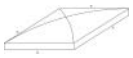						
▲ ▲ ▲ ▲ △ ▲ ▲ ▲ ▲ △ ▲ ▲ ▲ ▲ ▲	100.0	100.0	100.0	100.0	100.0	100.0
CPT	96.1	98.4	98.4	66.8	66.8	1974.2
FSDT	100.9	98.4	98.4	66.8	66.8	1974.2
Kant-2	99.9	100.3	100.3	100.0	100.0	79.4
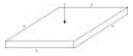						
□ ■ □ ■ □ □ ■ □ ■ □ ■ □ ■ □ ■	100.0	100.0	100.0	100.0	100.0	100.0
CPT	91.4	83.7	83.7	67.0	67.0	540.1
FSDT	99.9	83.7	83.7	67.0	67.0	540.1
Kant-2	100.0	96.5	96.5	99.9	99.9	39.5
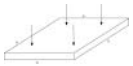						
▽ ▼ ▽ ▼ ▽ ▽ ▼ ▽ ▼ ▽ ▼ ▽ ▼ ▽ ▼	100.0	100.0	100.0	100.0	100.0	100.0
CPT	91.4	83.7	83.7	67.0	67.0	540.1
FSDT	99.9	83.7	83.7	67.0	67.0	540.1
Kant-2	100.0	96.5	96.5	99.9	99.9	39.5

6.3. Loading, Boundary Condition, and Thickness Effects

The combined effect of loading and boundary conditions is considered. The influence of the length-to-thickness ratio, a/h, is also investigated. The loading sets considered are the same as those seen in the previous analyses. Each output variable is associated to a symbol as shown in Table 15. A thin plate is first considered by assuming a/h equals 100. Table 16 shows the sets of displacement variables that are needed to detect various output variables previously. Each row refers to a different loading condition, each column to different boundary conditions. Table 17 reports the plate models that precisely detect all the considered outputs for all the considered boundary and loading conditions. Tables 18 to 21 report the same type of results for a/h equal to 10 and 5, respectively. The obtained plate models are summarized in Table 22 where all the considered a/h cases are shown. Table 23 presents a comparison of the accuracies given by the plate models obtained and the classical theories. A plate with two clamped and two free edges is considered. For the sake of brevity, the accuracy data which are related to the other boundary conditions are not reported here. Fig. 7 shows the total number of terms as function of the error and a/h. This plot has been obtained following the approach exploited for

TABLE 14
Sets of effective terms for the considered loading conditions

▲□▽	▲■▼	▲□▽	▲■▼	△ □▽
▲□▽	▲■▼	▲□▽	▲■▼	△ □▽
▲■▼	▲□▽	▲■▼	▲□▽	▲■▼

TABLE 15
Symbols that indicate the status of a displacement variable for different output variables

Active term	Inactive term	
▲	△	u_z
■	□	σ_{xx}
▼	▽	σ_{xz}
♦	◊	σ_{zz}

TABLE 16
Comparison of the sets of effective terms for plates with different boundary and loading conditions, $a/h = 100$. ▲ $= u_z$, ■ $= \sigma_{xx}$, ▼ $= \sigma_{xz}$ and ♦ $= \sigma_{zz}$

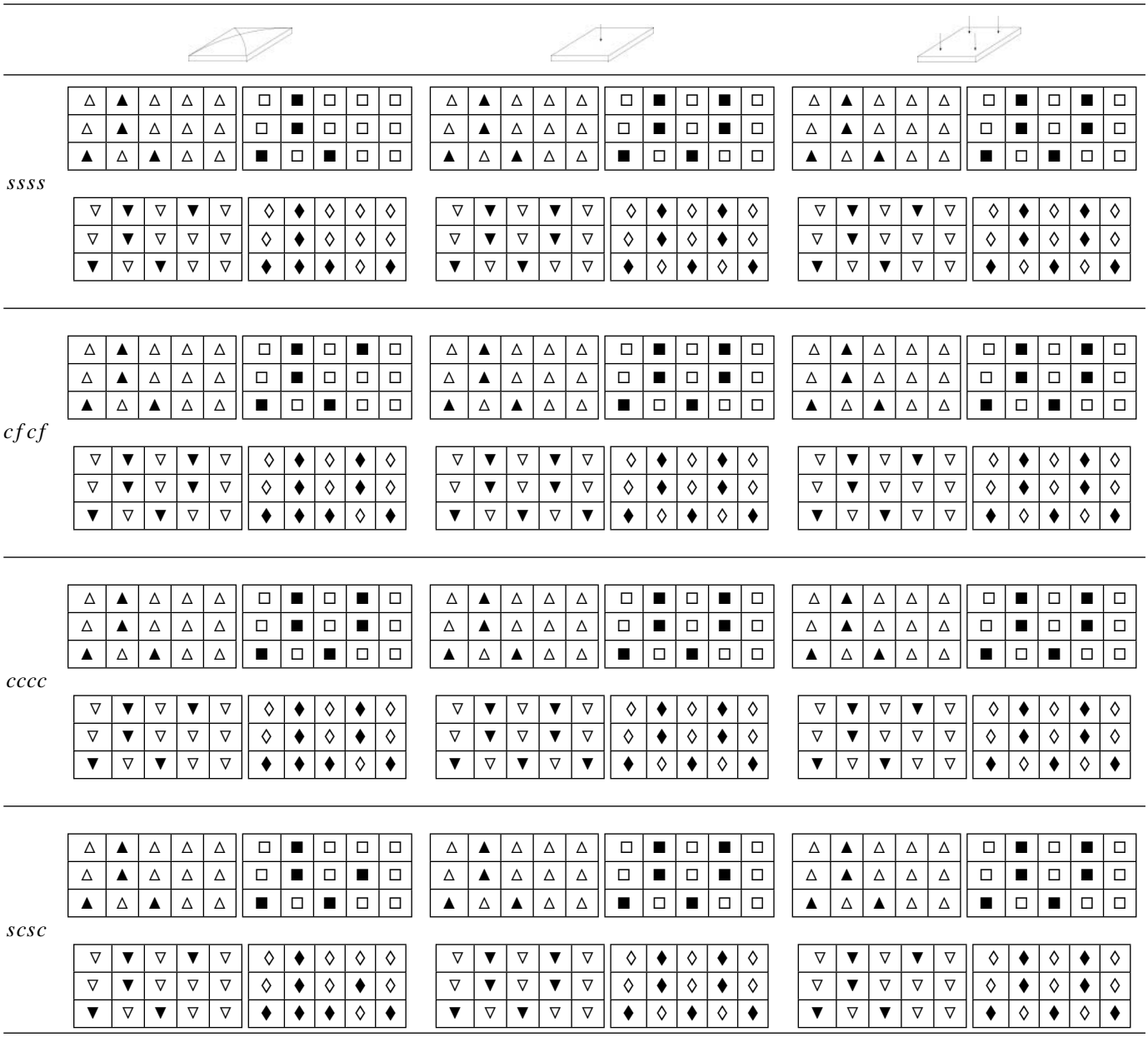

Figs. 3, 4, and 6. The analyses carried out suggest the following comments.

1. The sets of effective displacement variables depend on all the three considered parameters: loadings, boundary conditions, and thickness.
2. The proper analysis of thick plates require more sophisticated models since the total number of expansion terms increases as a/h decreases. This result is analogous to that in Carrera and Petrolo [37].
3. It is confirmed that different output variables require different plate models to be properly detected.

7. FINAL GUIDELINES ON BEST PLATE THEORIES

The effectiveness of higher-order plate theories is investigated in this paper. Refined models have been hierarchically obtained by means of the Carrera Unified Formulation, CUF. The finite element analysis has been used to deal with arbitrary geometries, loadings, and boundary conditions. Isotropic plates

TABLE 17

Sets of effective terms for the considered boundary and loading conditions, $a/h = 100$

△□▽◊	▲■▼♦	△ □▽◊	△■▼♦	△ □▽◊
△□▽◊	▲■▼♦	△ □▽◊	△■▼♦	△ □▽◊
▲■▼♦	△□▽♦	▲■▼♦	△ □▽◊	△□▼♦

TABLE 19

Sets of effective terms for all the considered boundary and loading conditions, $a/h = 10$

△ ■▽♦	▲■▼♦	△ □▽♦	▲■▼♦	△ □▽◊
△ ■▽♦	▲■▼♦	△ □▽♦	▲■▼♦	△ □▽◊
▲■▼♦	▲■▽♦	▲■▼♦	△ □▽♦	▲■▼♦

TABLE 18

Comparison of the sets of effective terms for plates with different boundary and loading conditions, $a/h = 10$. ▲ $= u_z$, ■ $= \sigma_{xx}$, ▼ $= \sigma_{xz}$ and ♦ $= \sigma_{zz}$

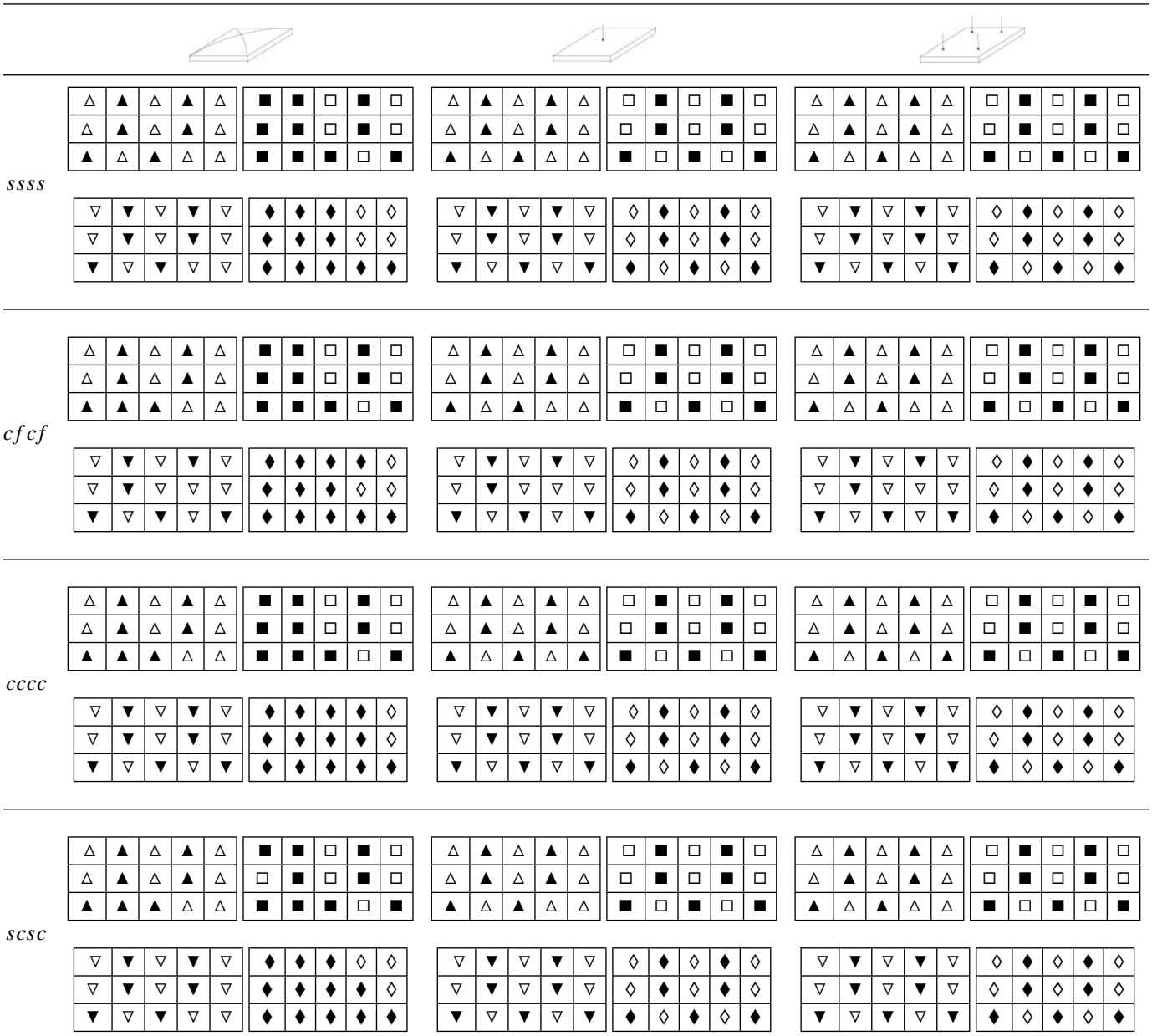

TABLE 20
Comparison of the sets of effective terms for plates with different boundary and loading conditions, $a/h = 5$, ▲ $= u_z$, ■ $= \sigma_{xx}$, ▼ $= \sigma_{xz}$ and ♦ $= \sigma_{zz}$

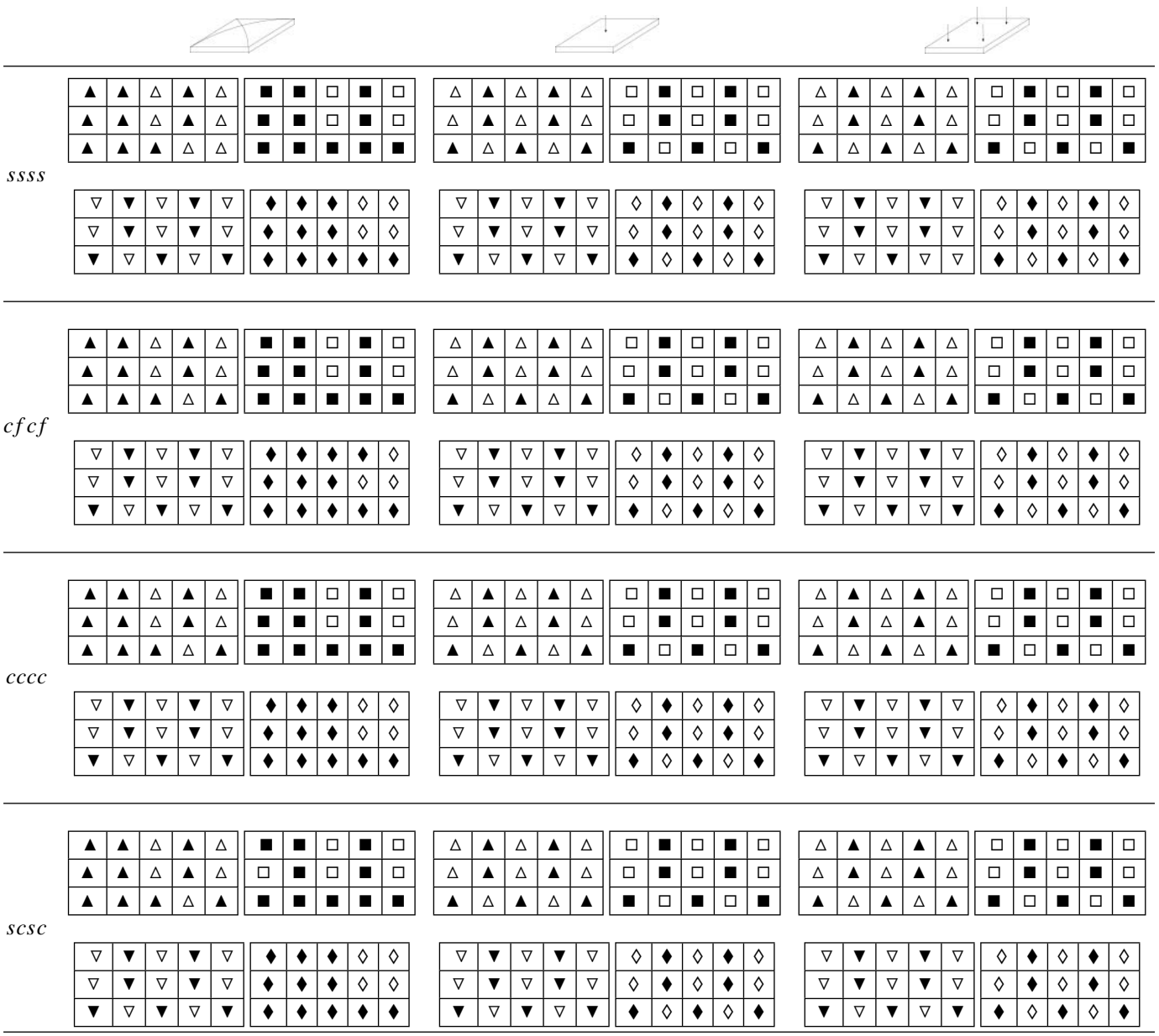

TABLE 21
Sets of effective terms for the considered boundary and loading conditions, $a/h = 5$

▲■▽♦	▲■▼♦	△ □▽♦	▲■▼♦	△ □▽◊
▲■▽♦	▲■▼♦	△ □▽♦	▲■▼♦	△ □▽◊
▲■▼♦	▲■▽♦	▲■▼♦	△ ■▽♦	▲■▼♦

have been considered. A fourth-order solution has been adopted as reference. The accuracy analysis has been conducted via a so-called mixed asymptotic/axiomatic approach, which determines the role of each displacement variable in computing a given displacement/stress variable. The present approach has proved its validity in constructing:

1. Reduced plate models equivalent to a full higher-order theory;
2. Reduced plate models able to fulfil a given accuracy input.

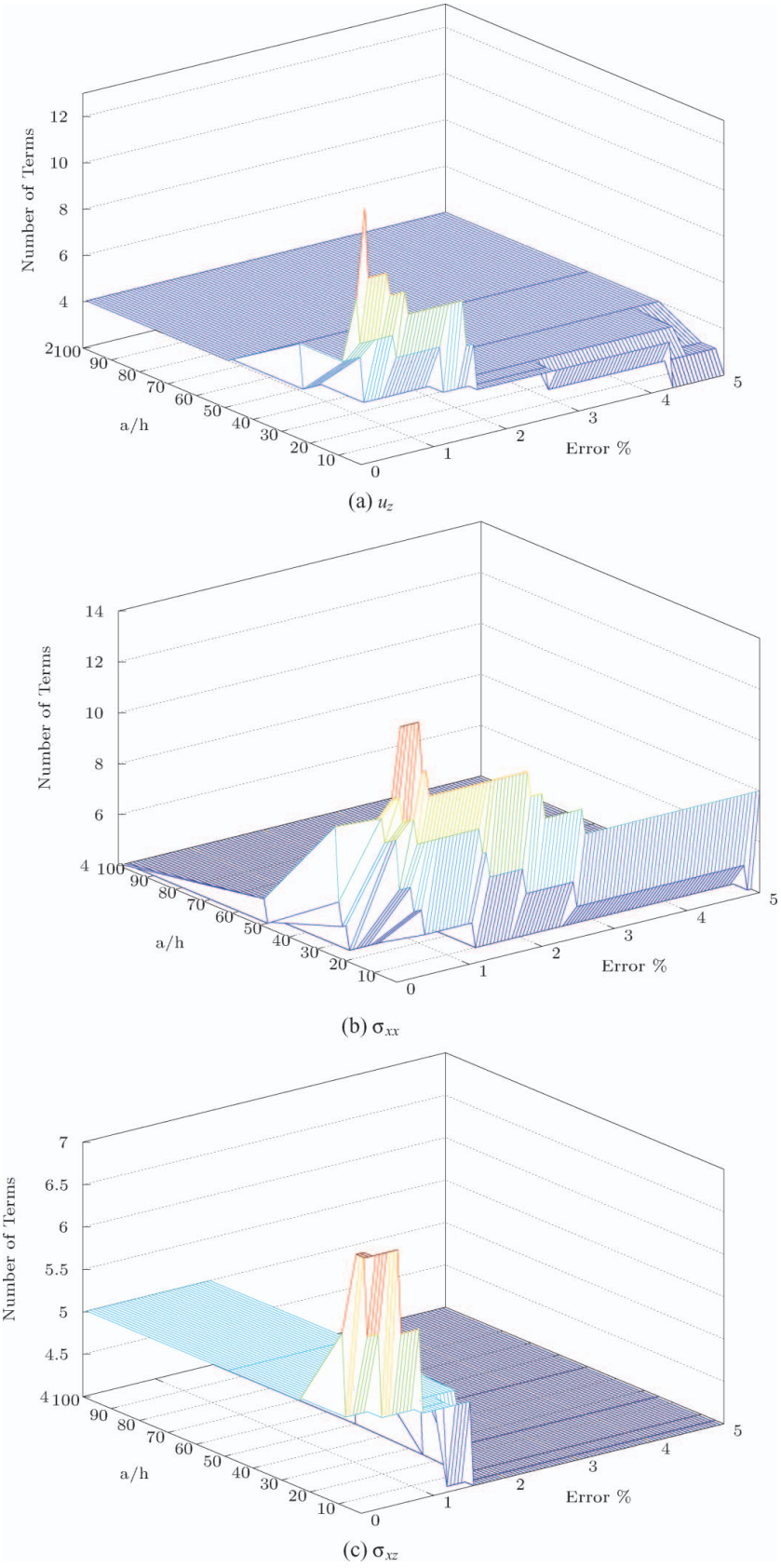

FIG. 7. Influence of a/h, the output variable, and the tolerance on the total number of model terms for a simply supported plate with a distributed load. (Color figure available online)

TABLE 22
Influence of a/h on the displacement field terms for combined boundary and loading conditions

$a/h = 100$	△ □▽◊	▲■▼♦	△ □▽◊	△■▼♦	△ □▽◊
	△ □▽◊	▲■▼♦	△ □▽◊	△■▼♦	△ □▽◊
	▲■▼♦	△□▽♦	▲■▼♦	△ □▽◊	△□▼♦
$a/h = 10$	△ ■▽♦	▲■▼♦	△ □▽♦	▲■▼♦	△ □▽◊
	△ ■▽♦	▲■▼♦	△ □▽♦	▲■▼♦	△ □▽◊
	▲■▼♦	▲■▽♦	▲■▼♦	△ □▽♦	▲■▼♦
$a/h = 5$	▲■▽♦	▲■▼♦	△ □▽♦	▲■▼♦	△ □▽◊
	▲■▽♦	▲■▼♦	△ □▽♦	▲■▼♦	△ □▽◊
	▲■▼♦	▲■▽♦	▲■▼♦	△ ■▽♦	▲■▼♦

As far as the first type of models is concerned, the following conclusions can be drawn:

- All the parameters considered (loadings, boundary conditions, and thickness) are important to determine the sets of effective terms; that is, as one of these parameters changes, a different plate model is required.
- The influence of the length-to-thickness ratio is particularly strong.
- The use of full models is mandatory when a complete set of results is needed, since only few can be discarded.

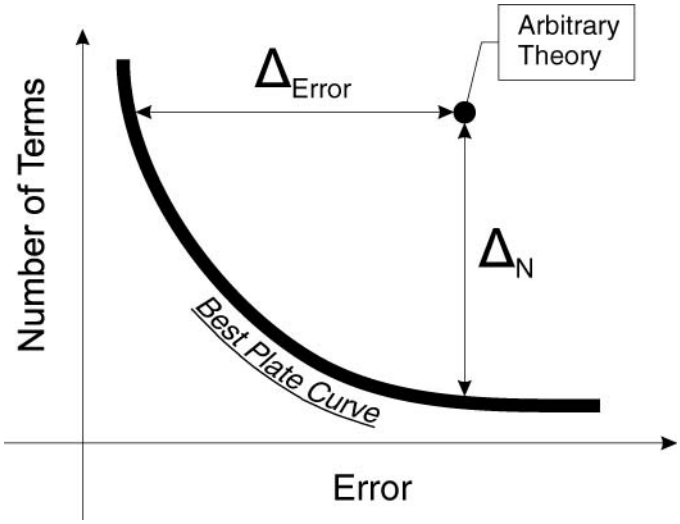

FIG. 8. An example of Best Plate Diagram (BPD).

TABLE 23
Accuracy of different displacement models in the case of a plate with two clamped and two free edges subject to a point load

	δ_{u_z} [%]	$\delta_{\sigma_{xx}}$ [%]	$\delta_{\sigma_{yy}}$ [%]	$\delta_{\sigma_{xz}}$ [%]	$\delta_{\sigma_{xz}}$ [%]	$\delta_{\sigma_{zz}}$ [%]
$a/h = 100$						
△ □▽◊ ▲■▼♦ △ □▽◊ △■▼♦ △ □▽◊ △ □▽◊ ▲■▼♦ △ □▽◊ △■▼♦ △ □▽◊ ▲■▼♦ △□▽♦ ▲■▼♦ △ □▽◊ △□▼♦	100.0	100.0	100.0	100.0	100.0	100.0
CPT	102.7	98.5	98.0	158.6	710.2	1337.4
FSDT	102.9	98.5	98.0	80.0	114.3	1337.6
Kant-2	100.0	100.0	100.0	99.9	117.9	99.0
$a/h = 10$						
△ ■▽♦ ▲■▼♦ △ □▽♦ ▲■▼♦ △ □▽◊ △ ■▽♦ ▲■▼♦ △ □▽♦ ▲■▼♦ △ □▽◊ ▲■▼♦ ▲■▽♦ ▲■▼♦ △ □▽♦ ▲■▼♦	100.0	100.0	100.0	100.0	100.0	100.0
CPT	86.2	82.5	79.2	202.9	−106.014	449.824
FSDT	101.6	82.7	80.24	83.6	72.7	453.2
Kant-2	100.0	96.2	95.7	98.7	97.7	39.8
$a/h = 5$						
▲■▽♦ ▲■▼♦ △ □▽♦ ▲■▼♦ △ □▽◊ ▲■▽♦ ▲■▼♦ △ □▽♦ ▲■▼♦ △ □▽◊ ▲■▼♦ ▲■▽♦ ▲■▼♦ △ ■▽♦ ▲■▼♦	100.0	100.0	100.0	100.0	100.0	100.0
CPT	60.7	70.6	65.7	228.9	−90.6	189.9
FSDT	102.8	70.9	68.1	88.7	71.6	193.5
Kant-2	100.4	89.7	88.7	96.0	99.1	−23.1

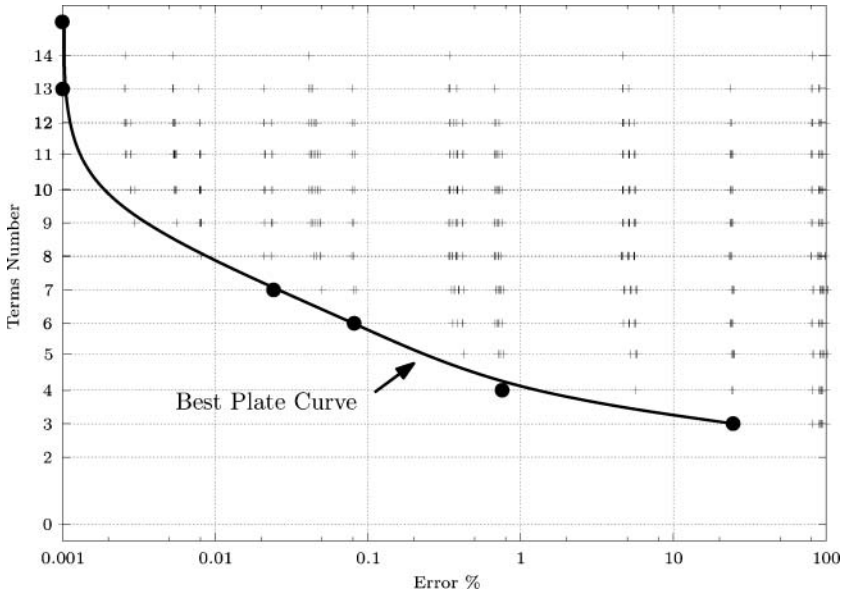

FIG. 9. Accuracy of all the possible combinations of plate models in computing u_z for the simply supported plate loaded by a distributed load (each "+" indicates a different plate model).

The construction of the second type of plate modes has highlighted that Unified Formulation allows us, for a given problem, to obtain a diagram that in terms of accuracy (input) gives an answer to the following fundamental questions (see Figs. 3, 4, and 6):

- What is the "minimum" number of the terms, N_{min}, to be used in a Finite Element Plate model?
- Which are the terms to be retained, that is, which are the generalized displacement variables to be used as FE dof's?

To the best of the authors' knowledge, there are no other available methods that can provide this kind of results. The present method of analysis is able to create plots like the one in Fig. 8 that gives the number of terms as function of the permitted error. This plot can be defined as Best finite element Plate Diagram, BPD, since it allows to edit an arbitrary given theory in order to have a lower amount of terms for a given error (vertical shift, Δ_N) or to increase the accuracy keeping the computational cost constant (horizontal shift, Δ_{error}). Most times, the plot presented appears as a hyperbole. CUF makes the computation of such a plot possible. Note that the diagram has the following properties:

- It changes by changing problems (a/h, loadings, boundary conditions, etc.);
- It changes by changing output variable (displacement/stress components, or a combination of these).

The validity of the BPD is tested by computing the accuracy of all the plate models obtainable as a combination of the 15 terms of the fourth-order theory. The results are reported in Fig. 9 in the case of a simply supported plate loaded by a distributed load, u_z is considered as output variable. The BPD perfectly matches the lower boundaries of the region where all the models lie. This confirms that the BPD represents the best theory (i.e. the least cumbersome) for a given error. The BPD permits the evaluation of any existing plate FE elements, as in the previous sections. The distance from the BPD of a given known FE model represents a guideline to recommend any other plate theory. More complex analyses will be conducted in future work to investigate the effects of the orthotropic ratio E_L/E_T, stacking sequence layout and variable kinematic description such as layer-wise or equivalent single layer models. Some of these analyses have been already studied in [37], where the attention was restricted to closed-form form solution.

REFERENCES

1. L. Euler, De Curvis Elasticis, Bousquet, Lausanne, 1744.
2. D. Bernoulli, De Vibrationibus et Sono Laminarum Elasticarum, Commentarii Academiae Scientiarum Imperialis Petropolitanae, vol. 13, pp. 105–120, 1751.
3. A. Cauchy, Sur l'Equilibre et le Mouvement d'une Plaque Solide, Exercises de Matematique, Vol. 3, pp. 328–355, 1828.
4. S. Poisson, Memoire Sur l'Equilibre et le Mouvement des Corps Elastique, Mem. Acad. Sci., Vol. 8, p. 357, 1829.
5. G. Kirchhoff, Uber das Gleichgewicht und die Bewegung Einer Elastishen Scheibe, J. Angew. Math., Vol. 40, pp. 51–88, 1850.
6. A.D. Saint-Venant, De la Torsion des Prismes, avec des Considérations sur leur Flexion, Ainsi que sur l'Équilibre des Solides Élastiques en Général, et des Formules Pratiques pour le Calcul de leur Résistance à Divers Efforts s'exerçant Simultanément, V. Dalmont, 1855.
7. A. E. H. Love, The Mathematical Theory of Elasticity, 4th ed., Cambridge University Press, Cambridge, 1927.
8. E. Reissner, The Effect of Transverse Shear Deformation on the Bending of Elastic Plates, Journal of Applied Mechanics, Vol. 12, pp. 69–76, 1945.
9. R. D. Mindlin, Influence of Rotatory Inertia and Shear in Flexural Motions of Isotropic Elastic Plates, Journal of Applied Mechanics, Vol. 18, pp. 1031–1036, 1951.

10. B. Vlasov, On the Equations of Bending of Plates, Dokla Ak Nauk Azerbeijanskoi-SSR, Vol. 3, pp. 955–979, 1975.
11. S. Ambartsumian Contributions to the theory of anisotropic layered shells, Appl. Mech. Rev., Vol. 15, pp. 245–249, 1962.
12. L. Librescu, and J. Reddy, A Critical Review and Generalization of Transverse Shear Deformable Anisotropic Plates, Euromech Colloquium 219, Kassel, Refined Dynamical Theories of Beams, Plates and Shells and Their Applications, pp. 32–43, Springer Verlag, Berlin, 1986.
13. E. Grigolyuk, and G. Kulikov, General Directions of the Development of Theory of Shells, Mekhanica Kompozitnykh Materialov, Vol. 24, pp. 287–298, 1988.
14. K. Kapania, and S. Raciti, Recent Advances in Analysis of Laminated Beams and Plates, Part I: Sheare Effects and Buckling, AIAA Journal, Vol. 27, No. 7, pp. 923–935, 1989.
15. K. Kapania, and S. Raciti, Recent Advances in Analysis of Laminated Beams and Plates, Part II: Vibrations and Wave Propagation, AIAA Journal, Vol. 27, No. 7, pp. 935–946, 1989.
16. K. Kapania, A Review on the Analysis of Laminated Shells, ASME J. Pressure Vessel Technol., Vol. 111, No. 2, pp. 88–96, 1989.
17. A. Noor, and W. Burton, Assessment of Shear Deformation Theories for Multilayered Composite Plates, Appl. Mech. Rev., Vol. 42, No. 1, pp. 1–18, 1989.
18. A. Noor, and W. Burton, Assessment of Computational Models for Multilayered Composite Shells, Appl. Mech. Rev., Vol. 43, No. 4, pp. 67–97, 1989.
19. A. Noor, W. Burton, and C. Bert, Computational Model for Sandwich Panels and Shells, Appl. Mech. Rev., Vol. 49, No. 3, pp. 155–199, 1986.
20. J. Reddy, and D. Robbins, Theories and Computational Models for Composite Laminates, Appl. Mech. Rev., Vol. 47, No. 6, pp. 147–165, 1994.
21. E. Carrera, Developments, Ideas and Evaluations Based Upon the Reissner's Mixed Variational Theorem in the Modeling of Multilayered Plates and Shells, Applied Mechanics Reviews, Vol. 54, pp. 301–329, 2001.
22. E. Carrera, Theories and Finite Elements for Multilayered Plates and Shells, Archives of Computational Methods in Engineering, Vol. 9, No. 2, pp. 87–140, 2002.
23. M. Qatu, Recent Research Advances in the Dynamic Behavior of Shells. Part 1: Laminated Composite Shells, Applied Mechanics Reviews, Vol. 55, No. 4, pp. 325–350, 2002.
24. M. Qatu, Recent Research Advances in the Dynamic Behavior of Shells. Part 2: Homogenous Shells, Applied Mechanics Reviews, Vol. 55, No. 5, pp. 415–434, 2002.
25. L. Librescu, Elasto-statics and Kinetics of Anisotropic and Heterogeneous Shell-Type Structures. Noordhoff Int, Leyden, Netherland, 1976.
26. J. Reddy, Mechanics of Laminated Composite Plates and Shells: Theory and Analysis, CRC Press, Boca Raton, FL, 2004.
27. M. Qatu, Vibration of Laminated Shells and Plates. Elsevier, Oxford, UK, 2004.
28. P. Cicala, Sulla Teoria Elastica della Parete Sottile, Giornale del Genio Civile, 4,6 and 9, 1959.
29. O. Fettahlioglu, and C. Steele, Asymptotic Solutions for Orthotropic Non-Homogeneous Shells of Revolution, ASME J. Appl. Mech., Vol. 44, pp. 753–758, 1974.
30. V. Berdichevsky, Variational Asymptotic Method of Shell Theory Construction. PMM, Vol. 43, pp. 664–667, 1979.
31. V. Berdichevsky, and V. Misyura, Effect of Accuracy Loss in Classical Shell Theory, Journal of Applied Mechanics, Vol. 59, pp. s217–s223, 1992.
32. D. Widera, and L. Logan, Refined Theories for Nonhomogeneous Anisotropic Cylindrical Shells: Part I-Derivation, Journal of the Engineering Mechanics Division, Vol. 106, No. 6, pp. 1053–1074, 1980.
33. D. Widera, and H. Fan, On the Derivation of a Refined Theory for Nonhomogeneous Anisotropic Shells of Revolution, ASME J. Appl. Mech., Vol. 110, pp. 102–105, 1988.
34. A.J.M. Spencer, P. Watson, and T.G. Rogers, Stress Analysis of Laminated Circular Cylindrical Shells 1990. Recent Developments in Composite Materials Structures, 1990. Presented at the Winter Annual meeting of ASME, Dallas, Nov., AD 19, AMD 113, ASME, New York, 1990.
35. P. Cicala, Systematic Approximation Approach to Linear Shell Theory. Levrotto e Bella, Torino, 1965.
36. A.L. Goldenweizer, Theory of Thin Elastic Shells, International Series of Monograph in Aeronautics and Astronautics, Pergamon Press, New York, 1961.
37. E. Carrera, and M. Petrolo, Guidelines and Recommendations to Construct Refinements of Classical Theories for Metallic and Composite Plates, AIAA Journal in Press.
38. M. Ganapathi, O. Polit, and M. Touratier, A c^0 Eight-Node Membrane-Shear-Bending Element for Geometrically Non-Linear (Static and Dynamic) Analysis of Laminates, International journal for Numerical Methods in Engineering Vol. 39, pp. 3453–3474, 1996.
39. O. Polit, and M. Touratier, High-order Triangular Sandwich Plate Finite Element for Linear and Non-Linear Analyses, Comput. Methods Appl. Mech. Engrg. Vol. 185, pp. 305–324, 2000.
40. M. Touratiert, and J. Faye, On a Refined Model in Structural Mechanics: Finite Element Approximation and Edge Effect Analysis for Axisymmetric Shells. Computers and Structures, Vol. 54, No. 5, pp. 897–920, 1995.
41. E. Carrera, and L. Demasi, Classical and Advanced Multilayerd Plate Elements Based Upon PVD and RMVT. Part 1: Derivation of finite element matrices, Int. J. Numer. Meth. Engng., Vol. 55, pp. 191–231, 2002.
42. E. Carrera, and L. Demasi, Classical and Advanced Multilayerd Plate Elements Based upon PVD and RMVT. part 2: Numerical implementation, Int. J. Numer. Meth. Engng., Vol. 55, pp. 253–291, 2002.
43. T. Kant, and K. Swaminathan, Estimation of Transverse/Interlaminar Stresses in Laminated Composites - a Selective Review and Survey of Current Developments. Composite Structures, Vol. 49, pp. 65–75, 2000.
44. E. Carrera, Historical review of Zig-Zag Theories for Multilayered Plates and Shells, Applied Mechanics Reviews, Vol. 56, pp. 287–308, 2003.
45. E. Carrera, Theories and Finite Elements for Multilayered Plates and Shells: a Unified Compact Formulation with Numerical Assessment and Benchmarking. Archives of Computational Methods in Engineering, Vol. 10, No. 3, pp. 216–296, 2003.
46. E. Carrera, and G. Giunta, Refined Beam Theories Based on Carrera's Unified formulation, International Journal of Applied Mechanics, Vol. 2, No. 1, pp. 117–143, 2010.
47. E. Carrera, and M. Petrolo, On the Effectiveness of Higher Order Terms in Refined Beam Theories, Journal of Applied Mechanics, vol. 78, No. 2, 2011.
48. E. Carrera, M. Cinefra, and P. Nali, Mitc Technique Extended to Variable Kinematic Multilayered Plate Elements Composite Structures, Composite Structures, vol. 92, No. 8, pp. 1888–1895, 2010.
49. E. Carrera, and S. Brischetto, Analysis of Thickness Locking in Classical, Refined and Mixed Theories for Layered Shells, Composite Structures, Vol. 85, pp. 83–90, 2008.
50. E. Carrera, and S. Brischetto, Analysis of Thickness Locking in Classical, Refined and Mixed Multilayered Plate Theories, Composite Structures, Vol. 82, pp. 549–562, 2008.
51. B. Pandya, and T. Kant, Finite Element Analysis of Laminated Compiste Plates Using High-Order Displacement Model, Composites Science and Technology, Vol. 32, pp. 137–155, 1988.
52. T. Kant, and B. Manjunatha, An Unsymmetric Frc Laminate c° Finite Element Model With 12 degrees of Freedom Per Node, Eng Comput, Vol. (5), No. 3, pp. 292–308, 1988.
53. T. Kant, Numerical Analysis of Thick Plates, Comput Meth Appl Mech Eng., Vol. 31, pp. 1–18, 1982.
54. E. Dvorkin, and K. Bathe, A Continuum Mechanics Based Four-Node Shell Element for General Nonlinear Analysis, Eng. Computations, Vol. 1, pp. 77–88, 1984.
55. E. Carrera, M. Cinefra, and P. Nali, Mitc Technique Extended to Variable Kinematic Multilayered Plate Elements, Composite Structures, Vol. 92, pp. 1888–1895, 2010.